STRATIGRAPHIC ASSESSMENT OF THE MINERAL AGGREGATE RESOURCES IN THE ST. BERNARD SHOALS, OFFSHORE LOUISIANA

Prepared for
U. S. Minerals Management Service
through
Bureau of Economic Geology
The University of Texas at Austin

by

Coastal Geoscience Laboratory
Center for Coastal, Energy, & Environmental Resources
Louisiana State University
E302 Howe-Russell Geoscience Complex
Baton Rouge, LA 70803
June 1993

David Pope
Paul Connor, Jr.
Shea Penland

DISCLAIMER

This report was prepared under contract 14-35-0001-30432 between U.S. Minerals Service (MMS) and the Center for Coastal, Energy & Environmental Resources (CCEER)-Coastal Geoscience Laboratory, formerly recognized as the Coastal Geology Section of the Louisiana Geological Survey (LGS). Although an internal peer review has been conducted, approval does not signify that the contents necessarily reflect the views and policies of MMS, nor does the mention of trade names of commercial products constitute endorsement or recommendation for use. This report is, however, exempt from review and compliance of MMS editorial standards.

TABLE OF CONTENTS

LIST OF FIGURES iv

ACKNOWLEDGEMENTS viii

INTRODUCTION 1

DATABASE 2
- Geophysical Database 2
- Geological Database 4

METHODOLOGY 6

HOLOCENE GEOLOGIC FRAMEWORK 11

ST. BERNARD SHOALS GEOMORPHOLOGY 14

ST. BERNARD SHOALS GEOLOGY 24
- Depositional Environments 24
- Geologic Cross Sections 31
- Isopach Mapping 31

SUMMARY AND CONCLUSIONS 32

REFERENCES CITED 34

APPENDIX 1-A 38

APPENDIX 1-B 46

APPENDIX 1-C 53

LIST OF FIGURES

Figure 1. Location of Holocene inner-shelf shoals formed on the Louisiana continental shelf (modified from Frazier 1974). 3

Figure 2. High-resolution seismic trackline chart and vibracore locations in St. Bernard Shoals region, Louisiana-Mississippi continental shelf. 5

Figure 3. Grain-size texture logs of vibracores CI-87-22 to CI-87-26. 7

Figure 4. Grain-size texture logs of vibracores CI-87-27 to CI-87-31. 8

Figure 5. Grain-size texture logs of vibracores CI-87-32 to CI-87-36. 9

Figure 6. Grain-size texture logs of vibracores CI-87-45 to CI-87-48, and CI-87-52. . . 10

Figure 7. Grain-size statistics (Moment, Folk, and Inman) of nineteen subsamples taken from vibracores located along St. Bernard Shoal. 13

Figure 8. Mass spectrometer analysis of vibracore CI-87-24, Run 1 at 2.2 meters subbottom. See Figure 2 for location of vibracore, and Appendix 1-A for mineralogic analysis of sample. 15

Figure 9. Mass spectrometer analysis of vibracore CI-87-24, Run 1 at 5.9 meters subbottom. See Figure 2 for location of vibracore, and Appendix 1-A for mineralogic analysis of sample. 16

Figure 10. Mass spectrometer analysis of vibracore CI-87-26, Run 1 at 0.4 meters subbottom. See Figure 2 for location of vibracore, and Appendix 1-A for mineralogic analysis of sample. 17

Figure 11. Mass spectrometer analysis of vibracore CI-87-26, Run 2 at 3.4 meters. See Figure 2 for location of vibracore, and Appendix 1-A for mineralogic analysis of sample. 18

Figure 12. Mass spectrometer analysis of vibracore CI-87-27, Run 1 at 0.4 meters subbottom. See Figure 2 for location of vibracore, and Appendix 1-A for mineralogic analysis of sample. 19

Figure 13. Mass spectrometer analysis of vibracore CI-87-30, Run 2 at 6.0 meters subbottom. See Figure 2 for location of vibracore, and Appendix 1-A for mineralogic analysis of sample. 20

Figure 14. Mass spectrometer analysis of vibracore CI-87-46, Run 1 at 0.2 meters subbottom. See Figure 2 for location of vibracore, and Appendix 1-A for mineralogic analysis of sample. 21

Figure 15. Isopach map of the St. Bernard Shoals. Note two major parallel shoal trends extending NE/SW. See Appendix 1-B for volumetric calculations of each sand shoal. Contour interval is 1 m. 23

Figure 16. Uninterpreted 3.5-kHz subbottom profile and line drawing of a sand shoal. Seismic profile acquired during CCEER/USGS 1989 Acadiana survey. See Figure 2 for location of profile. 26

Figure 17. Uninterpreted ORE geopulse boomer record and line drawing of a sand shoal. Seismic profile acquired during CCEER/USGS 1987 Acadiana survey. See Figure 2 for location of profile. 27

Figure 18. Schematic geologic cross sections A - A', B - B', and C - C'. Note flat bases of individual shoals, and their relationship to underlying distributary and/or tidal inlet systems. See Figure 20 for location of cross sections. . . . 28

Figure 19. A 100-kHz side-scan sonograph of sand shoal shown in Figure 8. Sonograph acquired during CCEER/USGS 1989 Acadiana survey. 29

Figure 20. Location of geologic cross sections A - A', B - B', and C - C. 30

ACKNOWLEDGEMENTS

This work was supported by the U. S. Mineral Management Service (Continental Margins Program) and built upon previous studies and field programs supported by the U.S. Geological Survey's National Coastal Geology Program. The Authors acknowledge the assistance and scientific discussion with J. Williams, J. Suter, M. Byrnes, and J. Kindinger. The recognition of M. Hiland for Intergraph support, and B. Blanchard and D. Murry for laboratory assistance is also deserved.

INTRODUCTION

The wetlands of the Mississippi River delta and chenier plains represent the largest deltaic estuary in North America, covering over 28,000 km^2. These wetlands are also undergoing the highest rates of coastal erosion and wetland loss in the U.S. (Coleman 1988; Penland 1990; Dunbar, Britch, and Kemp 1992). Average rates of land loss in the chenier plain of Louisiana approaches 21 km^2/yr, and almost 60 km^2/yr are lost in the delta plain (Dunbar et al. 1992). Such high rates of erosion and wetland loss pose serious long-term environmental, economic, and social consequences of local, state, and national importance (Craig et al. 1980; Barth and Titus 1984; Titus 1987; Penland et al. 1990).

Understanding natural processes and human-induced impacts that affect barrier island erosion, estuarine deterioration, and wetland loss in Louisiana is essential to proper development and evaluation of management strategies for wetlands restoration and protection. In 1981, the Louisiana state legislature established a Coastal Environmental Trust Fund, and mandated the implementation of a Coastal Protection Master Plan. Phase 1 of the Master Plan called for restoration of eroding barrier shorelines, while Phase 2 provides for beach replenishment using sand resources available from the Louisiana continental shelf (Jones and Edmonson 1987; Penland et al. 1989, 1990).

In 1983, research personnel at the Louisiana Geological Survey (LGS) and Louisiana State University (LSU) began a cooperative study with the U.S. Geological Survey (USGS) to inventory and assess known sand resources on the Louisiana continental shelf. To date, Approximately 17,500 line-km of high-resolution seismic profiles, and 625 vibracores have been acquired under this cooperative research program. Much effort has been focused on sand shoals of Holocene age including Trinity and Tiger Shoal, Ship Shoal, Outer Shoal, and St. Bernard Shoals (Figure 1). Preliminary studies have also been conducted to examine possible adverse

environmental impacts associated with sand dredging, particularly the effects that changes in seafloor bathymetry may have on normal wave refraction patterns approaching the shoreline (Mossa 1988; Suter et al. 1989; Byrnes and Patnaik 1991; Byrnes et al. 1991).

This report describes the results of an assessment of sand resources of the St. Bernard Shoals, and it examines the Holocene geologic framework of the St. Bernard Shoals region on the Louisiana-Mississippi continental shelf. These shoals are located about 30 km southeast of the Chandeleur Islands, and lie in 14 to 26 m of water (Figure 1). About 1300 line-km of high-resolution seismic profiles and side-scan sonographs acquired during 1982, 1987, and 1989 were interpreted and integrated with 20 vibracores collected during 1987 (Figure 2). From analysis of this data, the distribution, configuration, geometry, and thickness of the St. Bernard Shoals were mapped, and the approximate sand volume contained within each shoal was calculated. The mineralogy and textural characteristics of subsamples obtained from key vibracores were also determined through visual examination and statistical grain size analyses.

DATABASE

Geophysical Database

The high-resolution geophysical database used in this study consists of about 1300 line-km of data gathered during three separate surveys (Figure 2). These data sets include: (1) approximately 700 line-km of 3.5-kHz transducer and 400 Joule single-channel minisparker profiles filtered at 200 to 2000 Hz frequencies. These data were gathered by the USGS during the R/V *Gyre* 1981 survey on a NW/SE and NE/SW 5.5 km grid spacing (Kindinger et al. 1982). Navigation was accomplished using an integrated system of Loran-C, and Gyro compass. Shot points were marked on the seismic records every 300 m in real time; (2) approximately 400

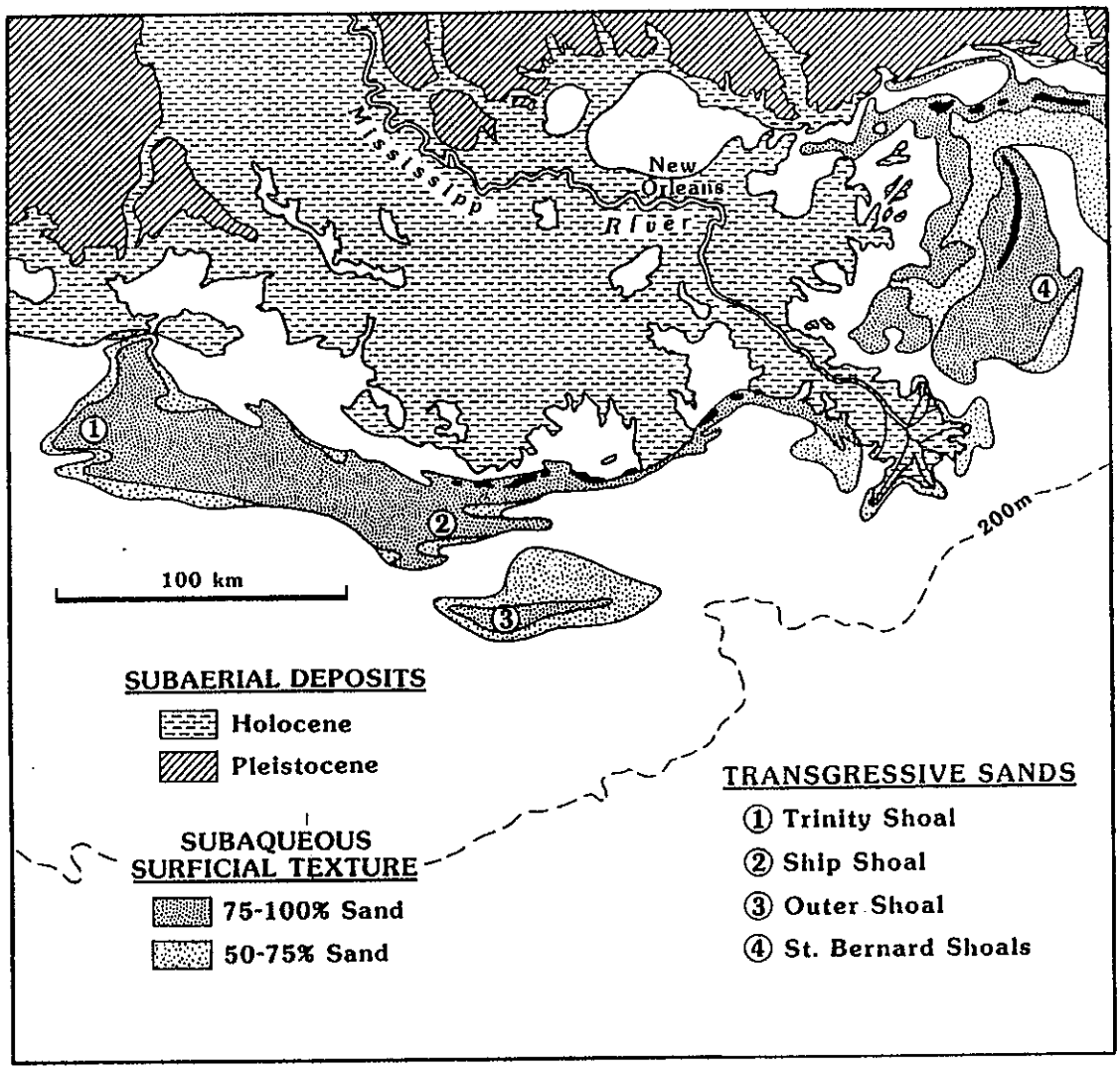

Figure 1. Location of Holocene inner-shelf shoals formed on the Louisiana continental shelf (modified from Frazier 1974).

line-km of 5-kHz transducer and ORE geopulse boomer profiles filtered at 300 to 800 Hz frequencies. These data were gathered by LSU/USGS during the R/V *Acadiana* 1987 survey on an irregular grid spacing. The returning signals were split-traced on an EPC 3200 recorder at sweep rates of 0.125 sec for each channel, resulting in an effective display of 0.25 sec for the entire record. All data were recorded on a Hewlett Packard 4300 reel-to-reel recorder for subsequent playback. Navigation was accomplished using a Northstar 600 Loran-C receiver, GPS, and a Morrow XYP-200 real time Loran plotter. The navigation data were recorded on magnetic tape using a Texas Instruments Silent 700 and processed into trackline charts by the USGS. Navigation shot points were marked on the seismic records every 5 minutes in real time; and (3) approximately 150 line-km of 3.5-kHz transducer, 300 to 800 Hz ORE geopulse boomer profiles, and 100 to 500-kHz variable frequency side-scanning sonar. These data were gathered by LSU/USGS aboard the R/V *Acadiana* 1989 survey on a NE/SW grid, intersected by a N/S and E/W irregular grid spacing. The side-scan sonographs were recorded on an EG&G Model 260 Image Correcting recorder. Range settings were generally set at 100 m on the 100-kHz frequency, resulting in a 200 m total swath range for each line. The seismic profiles and navigation data were recorded and processed in the same manner as the R/V *Acadiana* 1987 survey data described above.

Geological Database

The geological database used in this study consists of 20 vibracores acquired by the LSU/USGS during 1987 aboard the R/V *Blue Streak* (Figures 2 and 3 - 6). Vibracoring is a sampling technique that uses a pneumatic vibrating core barrel to achieve penetration through sea-bottom sediments. This coring technique usually preserves sedimentary structures contained within the core barrel better than other coring methods. The vibracore samples were collected

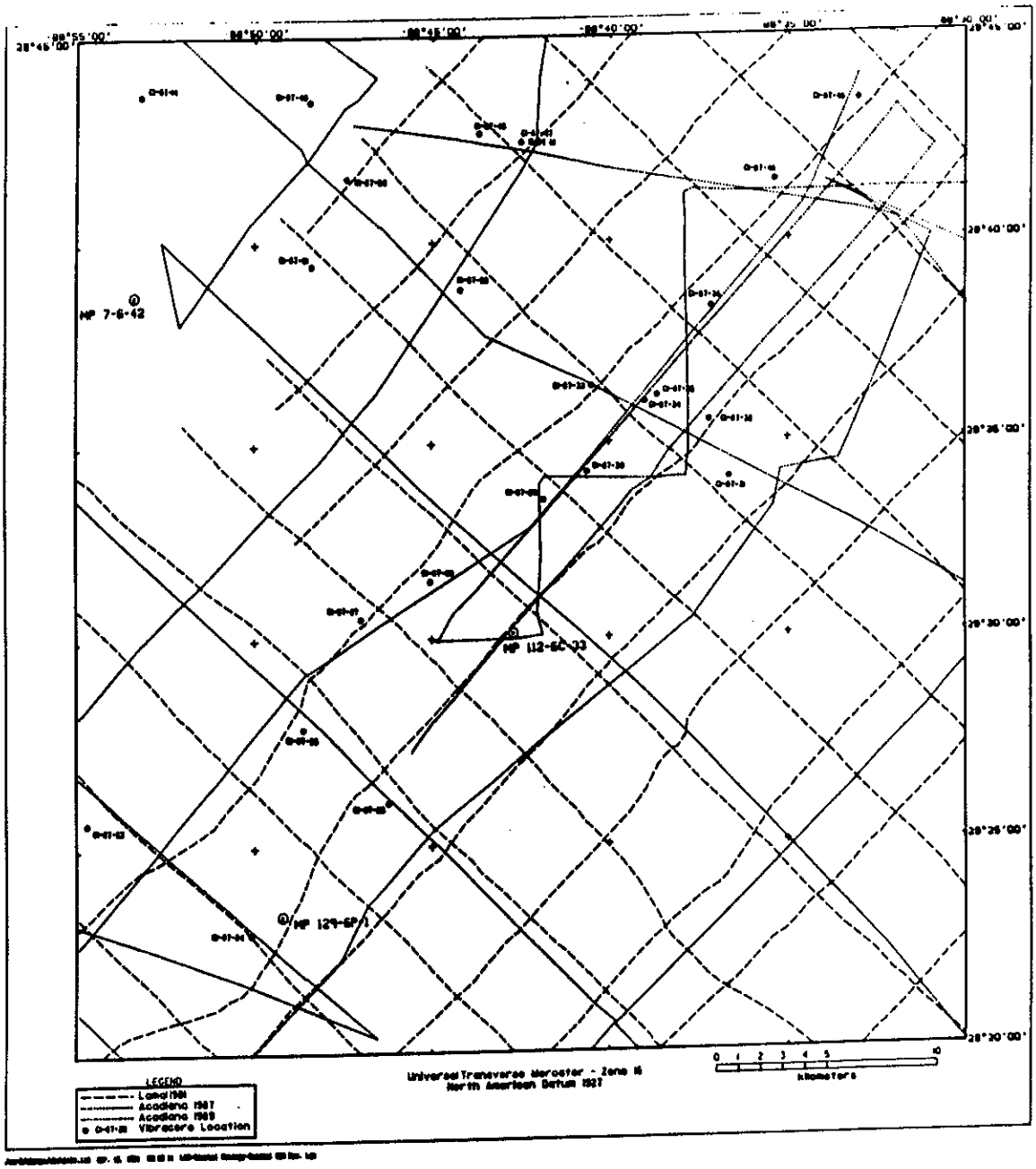

Figure 2. High-resolution seismic trackline chart and vibracore locations in St. Bernard Shoals region, Louisiana-Mississippi continental shelf.

using a 10.36 cm outside diameter by 9.32 m long fiberglass core barrel. To achieve maximum penetration, each vibracore was acquired by implementing two coring runs. The first run was cored to maximum penetration and then extracted. The second run was achieved by using a high-pressure water drive system to jet down to within 1 m of the bottom of the first core run, and again cored to maximum penetration. Total vibracore lengths varied between 10 and 12 m. Sediment compaction (consolidation) within each vibracore was greatest near the seafloor interface (.50 to 1.25 m), and decreased with down hole penetration. The vibracores were then capped, labeled, and transported back to the lab for analysis.

METHODOLOGY

Exploration for offshore sand resources in the St. Bernard Shoals region was conducted in two separate phases. The first phase involved seismic acquisition, and the second phase involved vibracoring. Vibracore locations were chosen from preliminary interpretation of the seismic data. Following acquisition of the seismic profiles and vibracores, core locations and navigation shot points from each survey were digitized into an Intergraph Interview 32c workstation, and plotted on mylar overlays on a Hewlett Packard 7595 plotter at a scale of 1:80,000. All tracklines were numbered consecutively for each survey, and shot points were plotted in real time. Each data set and acoustic source were interpreted separately and then integrated to evaluate and calibrate the various seismic systems, acquisition vintages, and processing techniques.

The textural suitability of St. Bernard Shoals as an aggregate resource was determined by grain-size analysis of nineteen subsamples obtained from vibracores located within the study site (Figure 7). Seven additional subsamples form six vibracores were analyzed for their mineralogy by mass spectrometer (Figure 8 - 14 and Appendix 1-A). After completing core

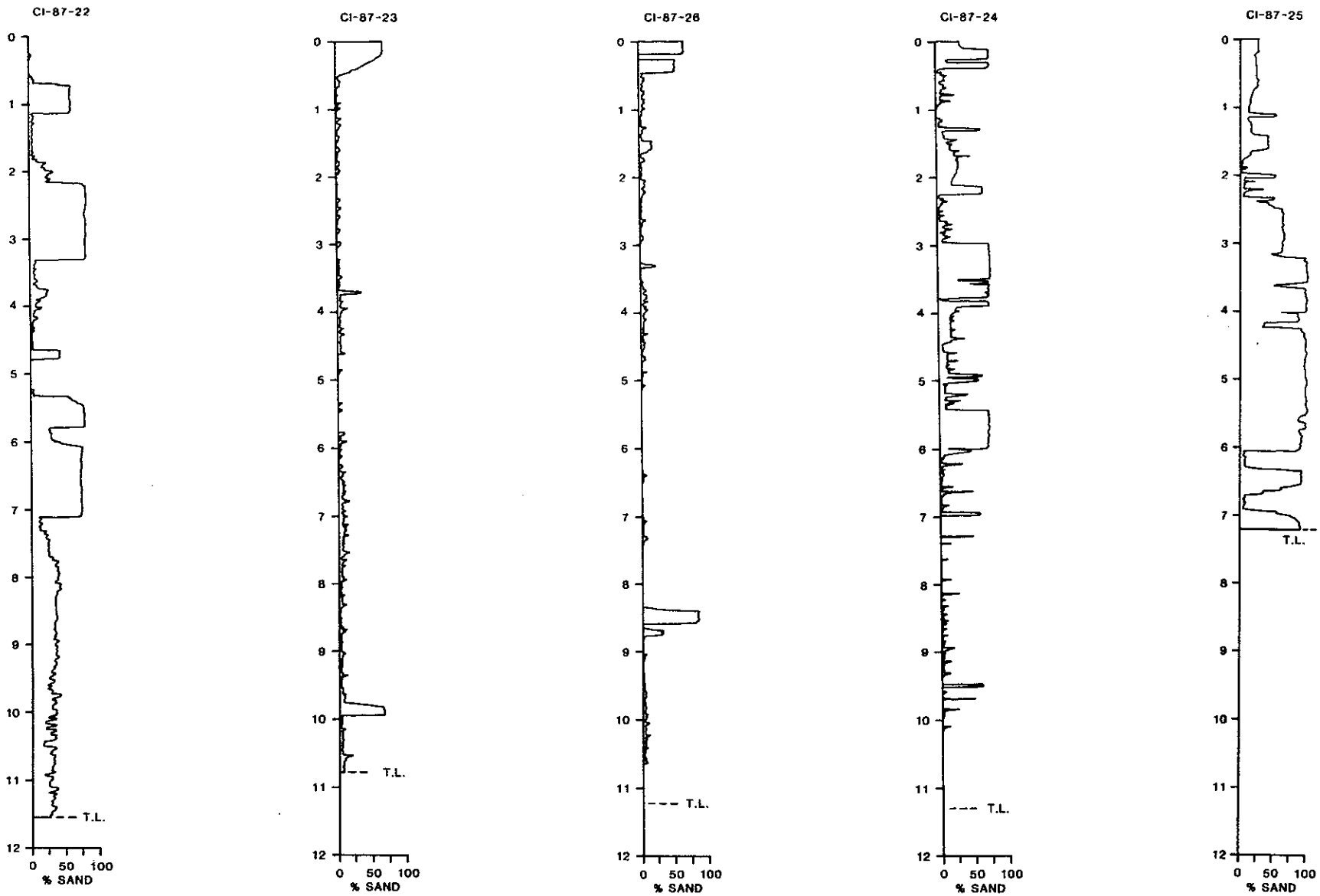

Figure 3. Grain-size texture logs of vibracores CI-87-22 to CI-87-26.

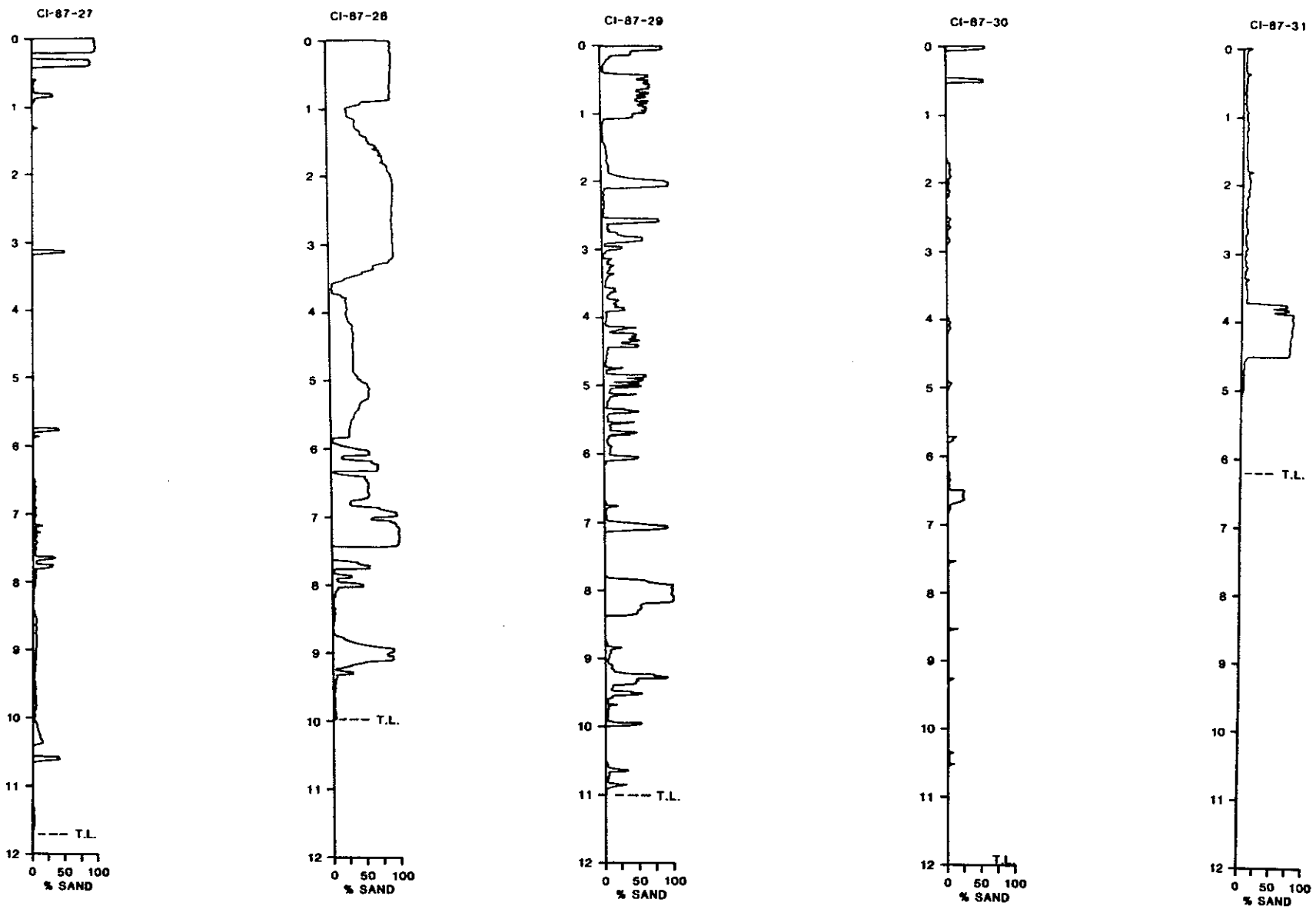

Figure 4. Grain-size texture logs of vibracores CI-87-27 to CI-87-31.

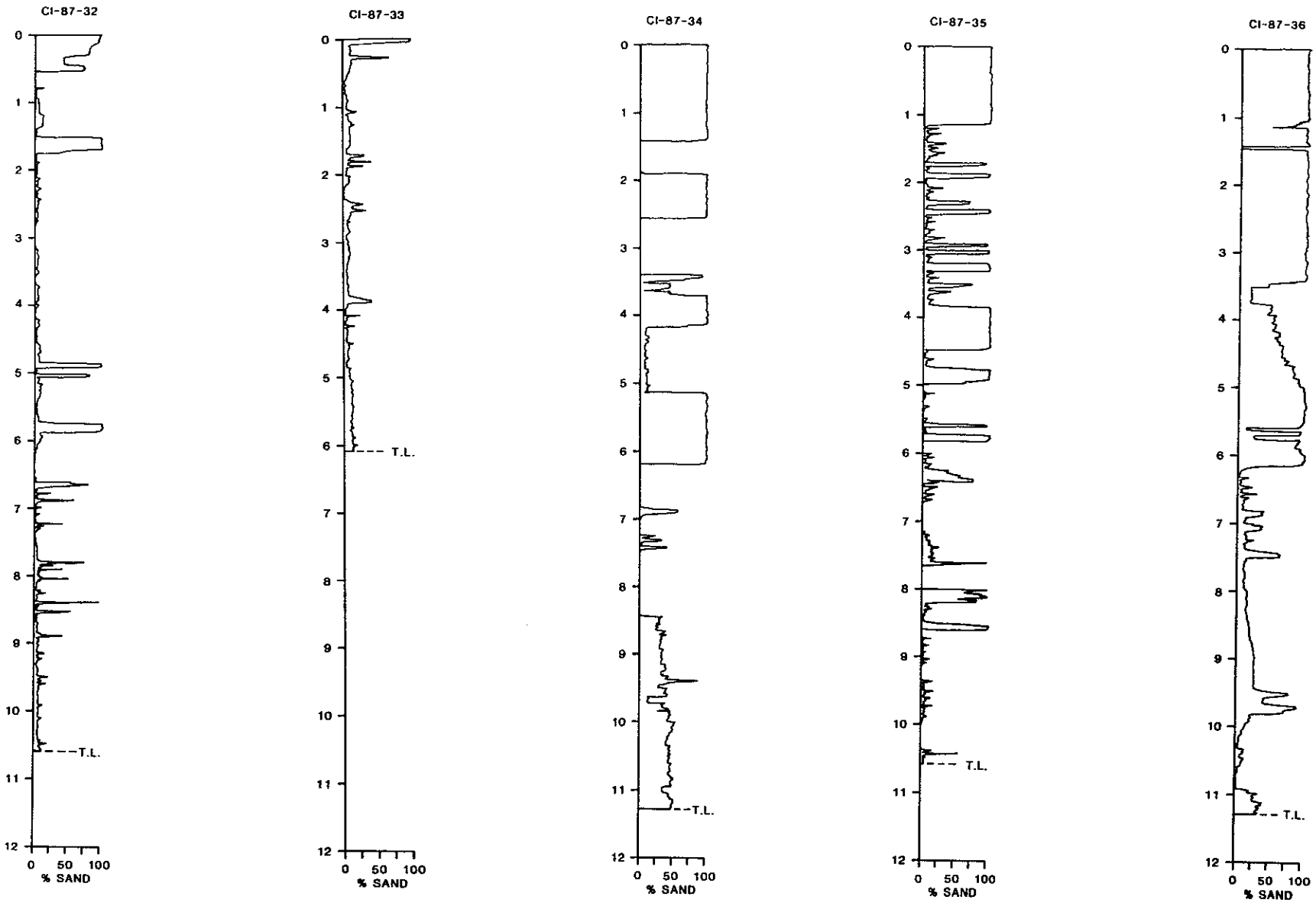

Figure 5. Grain-size texture logs of vibracores CI-87-32 to CI-87-36.

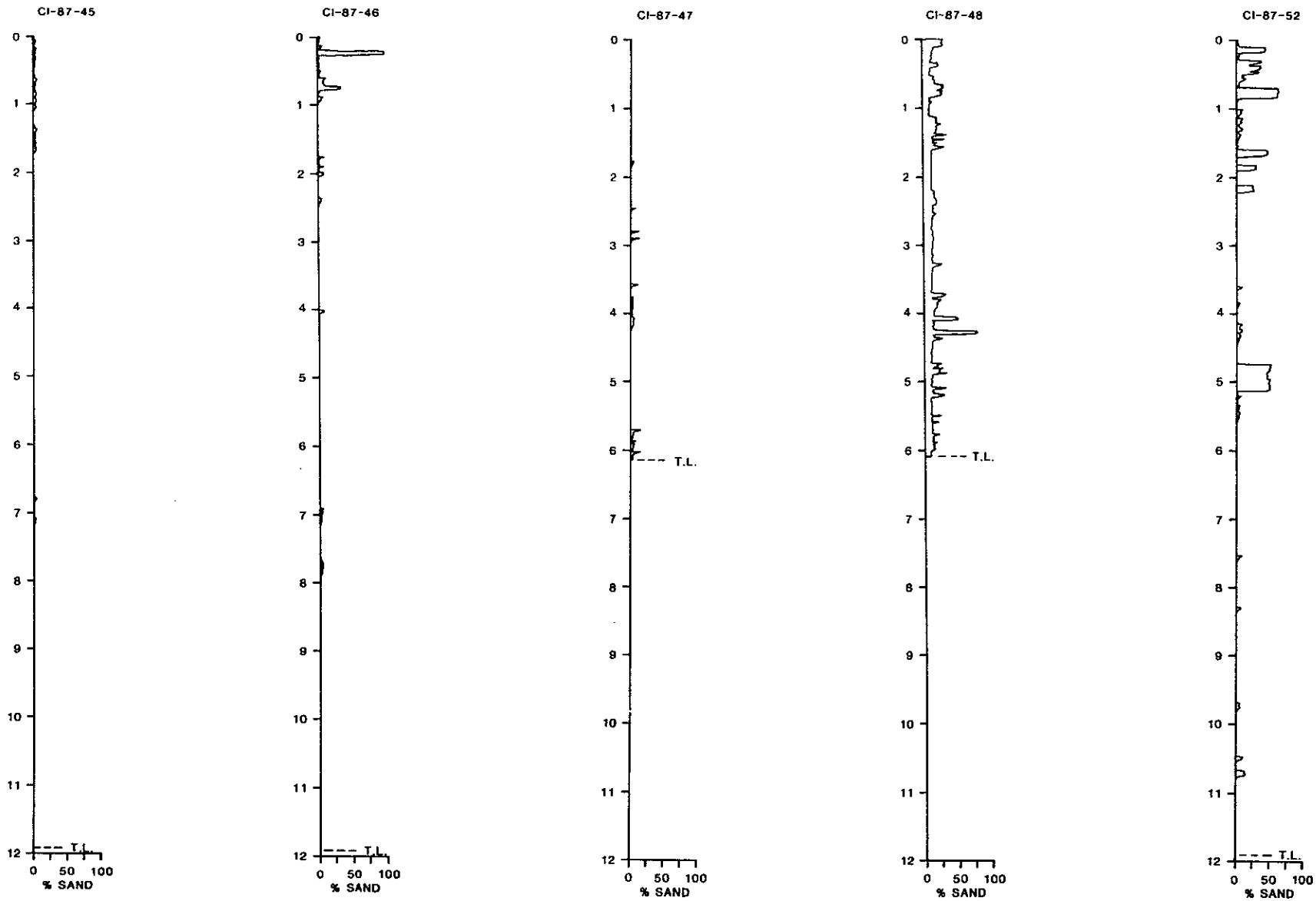

Figure 6. Grain-size texture logs of vibracores CI-87-45 to CI-87-48, and CI-87-52.

descriptions and textural analyses, core data were integrated with the seismic profiles to calibrate and classify the seismic facies character of the sand shoals. Sand shoal seismic facies were classified by their internal reflection character and external geometries as described by Mitchum et al. (1977), and calibrated to available borings. This procedure allowed a direct correlation between the sand shoals and their seismic character, and a regional interpretation of these seismic facies in terms of the geologic setting and depositional processes. Depositional processes were inferred primarily on the distribution of these geometries, and through review of previous studies (Kolb and Van Lopik 1958; Ludwick 1964; Frazier 1967, 1974; Coleman 1976; Mazullo and Bates 1985; Kindinger 1988).

An isopach map and three schematic geologic cross sections were also constructed to illustrate the shoals distribution, configuration, geometry, and thickness trends of sand resources throughout the region. The isopach map and geologic cross sections were also used to interpret the geologic processes responsible for the origin of the shoals. Volumetric calculations of sand contained within each individual shoal were determined by calculating the area between each 2 m contour interval using the following formula:

Volume = Area 1 - Area 2 / 2 x Thickness.

HOLOCENE GEOLOGIC FRAMEWORK

The late Quaternary stratigraphic framework of the northern Gulf of Mexico was formed under the combined effects of sea level fluctuations and cyclic deltaic processes. During the last sea level lowstand about 18,000 yBP, sea level fell approximately 130 m below present levels, exposing the continental shelf and allowing rivers and coastal plain systems to prograde seaward

+ down cutting

creating a localized regression. Rates of progradation were enhanced by absolute sea level fall as continental glaciation removed water from the oceans (Fisk 1944; Curray 1960; Frazier 1967, 1974; Suter et al. 1987, 1991). The Mississippi River and other smaller river systems incised alluvial valleys and trenches across the shelf, depositing a series of shelf margin deltas near the edge of the continental shelf (Suter and Berryhill 1985; Coleman and Roberts 1991). During this low phase of sea level, an erosional unconformity was formed on the Pleistocene Prairie terrace, marked by incised valleys and a widespread oxidation surface formed by subaerial weathering processes (Fisk 1944).

Beginning about 9,000 yBP, a series of shelf-phase delta plains began forming as the site of major sedimentation shifted landward in response to the Holocene rise in sea level (Penland et al. 1988). Individual shelf-phase delta plains were formed as the rate of sea level rise slowed or achieved a stillstand. During periods of rapid relative sea level rise, delta plains undergo coastal submergence and land loss. This trend of transgression and submergence is reversed when the rate of rise drops below a critical threshold value (< 2 cm/yr) (Penland et al. 1991). The timing of delta formation is tied to each stillstand, backstepping as that threshold value is exceeded.

Each shelf-phase delta plain lies on a ravinement surface and consists of a regressive and transgressive component (Penland et al. 1988). During the regressive phase, distributary channels prograde seaward, and overbank sedimentation fills the shallow interdistributary bays. Through lateral migration of upper delta channels, overbanking, and dispersal processes at river mouths, a wide variety of sand bodies are deposited. The major sand bodies include fluvial channel-fill, bay-fill, distributary channel-fill, distributary mouth bar, and delta front environments (Coleman and Roberts 1991).

After abandonment, the subaerial delta undergoes a period of deterioration. The uppermost parts of the regressive phase deposits are reworked by marine processes, forming relatively thin transgressive deposits. During periods of high sea level, sedimentation on the shelf is characterized by thin, slowly accumulated calcareous-rich sequences, referred to as condensed sections. Condensed sections display high lateral continuity and a high amplitude acoustic response (Coleman and Roberts 1988, 1988a). Landward, transgressive deposits consist of lagoonal facies overlain by a barrier shoreline or shelf sand body. Sedimentation during periods of low sea level is characterized by rapidly accumulated coarse-grained sediment of variable thickness, referred to as expanded sections. Coarse-grained clastics include abundant sand and gravel deposited in well-defined depositional trends, and display a wide variety of acoustic response (Coleman and Roberts 1988, 1988a).

ST. BERNARD SHOALS GEOMORPHOLOGY

The St. Bernard Shoals are the easternmost member of an inner-shelf group of sand shoals that formed on the Louisiana continental shelf during the Holocene transgression. These shoals are located in 14 to 26 m of water on the Louisiana-Mississippi shelf, which forms a broad, gently sloping (< 1°) platform east of the Mississippi River delta (Kindinger 1988) (Figure 1).

The St. Bernard Shoals form a group of individual shoals that are part of a larger sand body approximately 45 km long and 10 to 15 km wide (Figure 15) (Penland et al. 1989). The shoals are generally asymmetrical to hummocky in profile (Figures 16 - 18); slopes on the shoal face reach 3° to 5° (1:17 to 1:20) on the lee side of individual shoals, and average 1:1,200 to 1:1,800 on the shoal crests. The shoal face slope direction of each shoal is extremely variable, but most commonly dip towards the SE (seaward), with gentler slopes on the shoal crest dipping

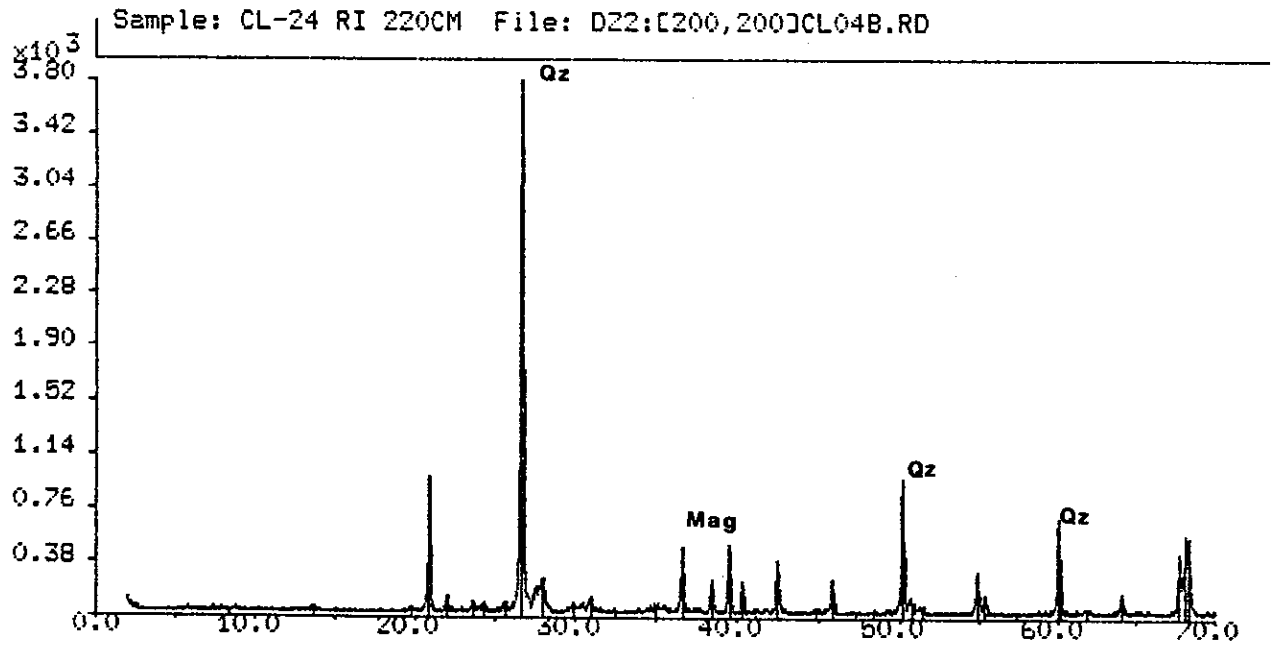

Figure 8. Mass spectrometer analysis of vibracore CI-87-24, Run 1 at 2.2 meters subbottom. See Figure 2 for location of vibracore, and Appendix 1-A for mineralogic analysis of sample.

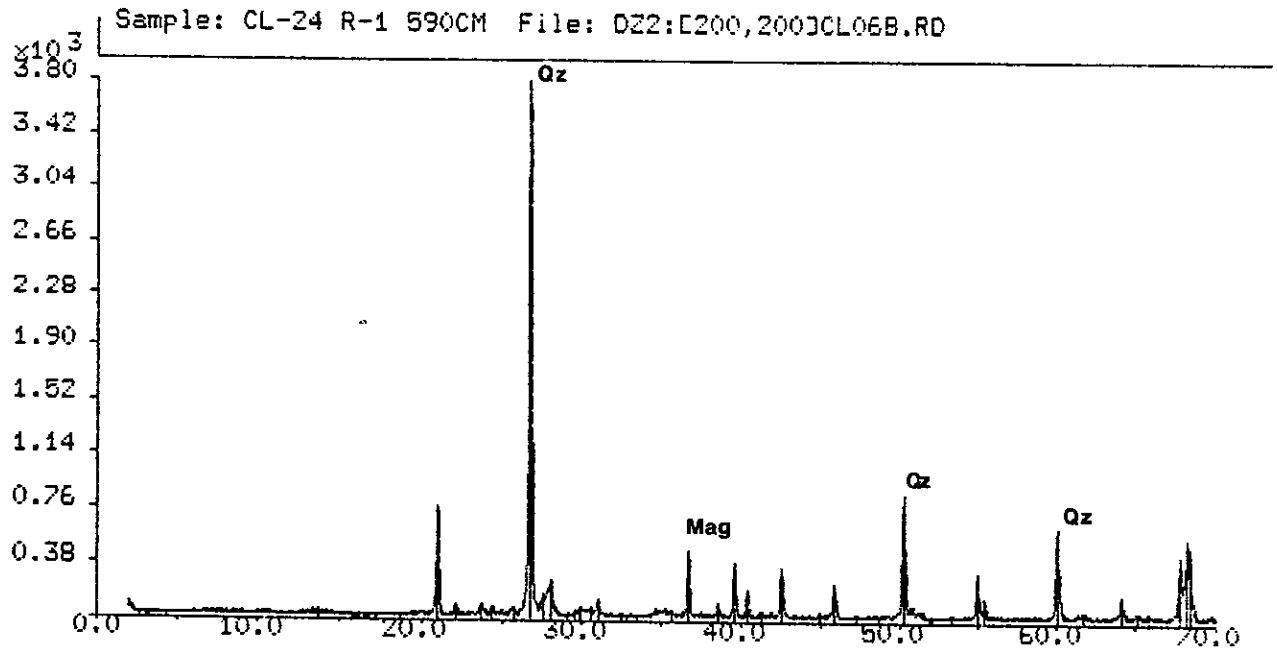

Figure 9. Mass spectrometer analysis of vibracore CI-87-24, Run 1 at 5.9 meters subbottom. See Figure 2 for location of vibracore, and Appendix 1-A for mineralogic analysis of sample.

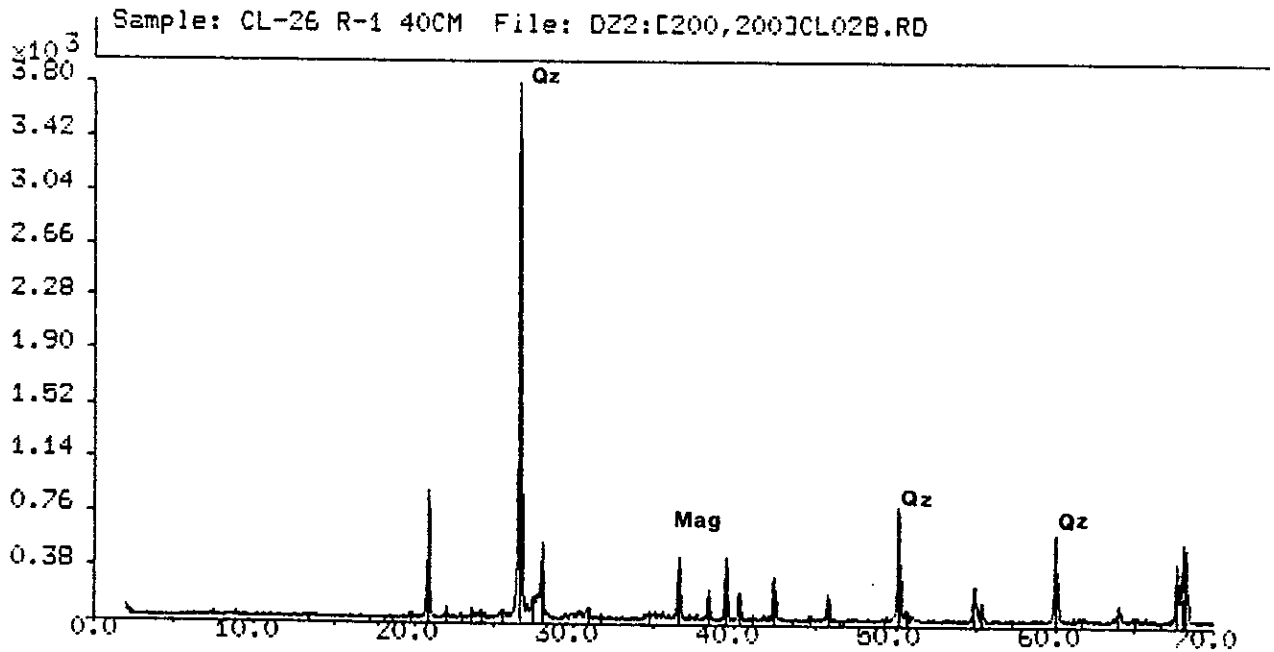

Figure 10. Mass spectrometer analysis of vibracore CI-87-26, Run 1 at 0.4 meters subbottom. See Figure 2 for location of vibracore, and Appendix 1-A for mineralogic analysis of sample.

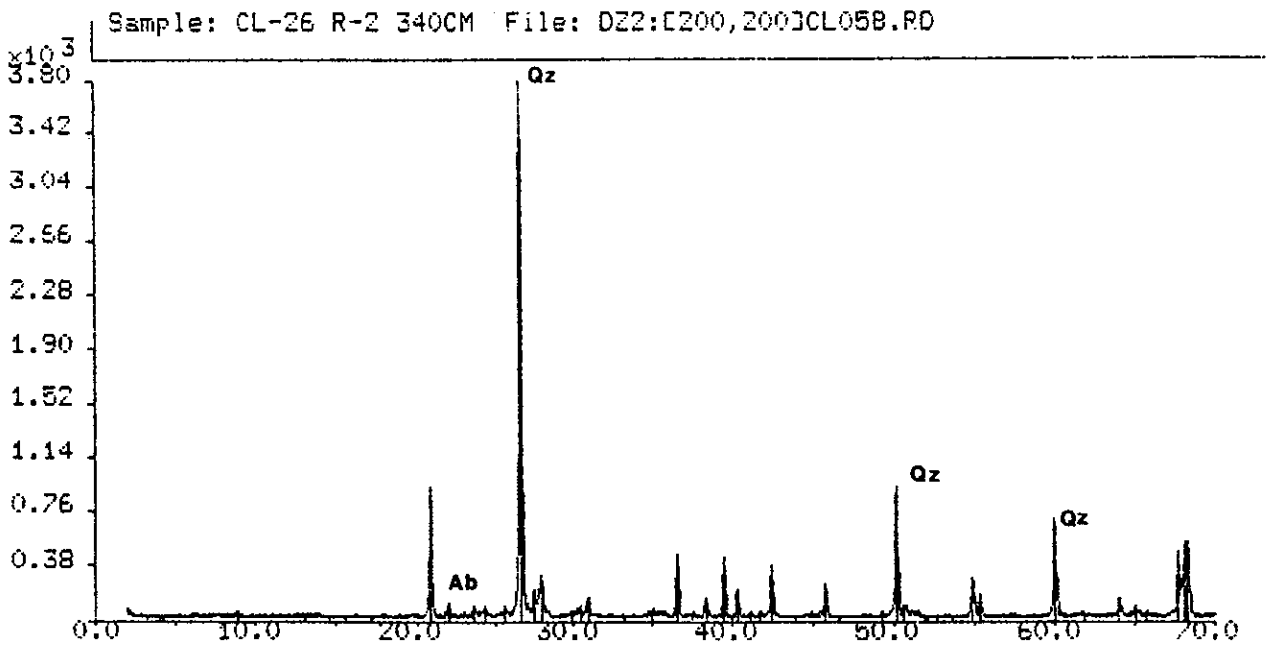

Figure 11. Mass spectrometer analysis of vibracore CI-87-26, Run 2 at 3.4 meters. See Figure 2 for location of vibracore, and Appendix 1-A for mineralogic analysis of sample.

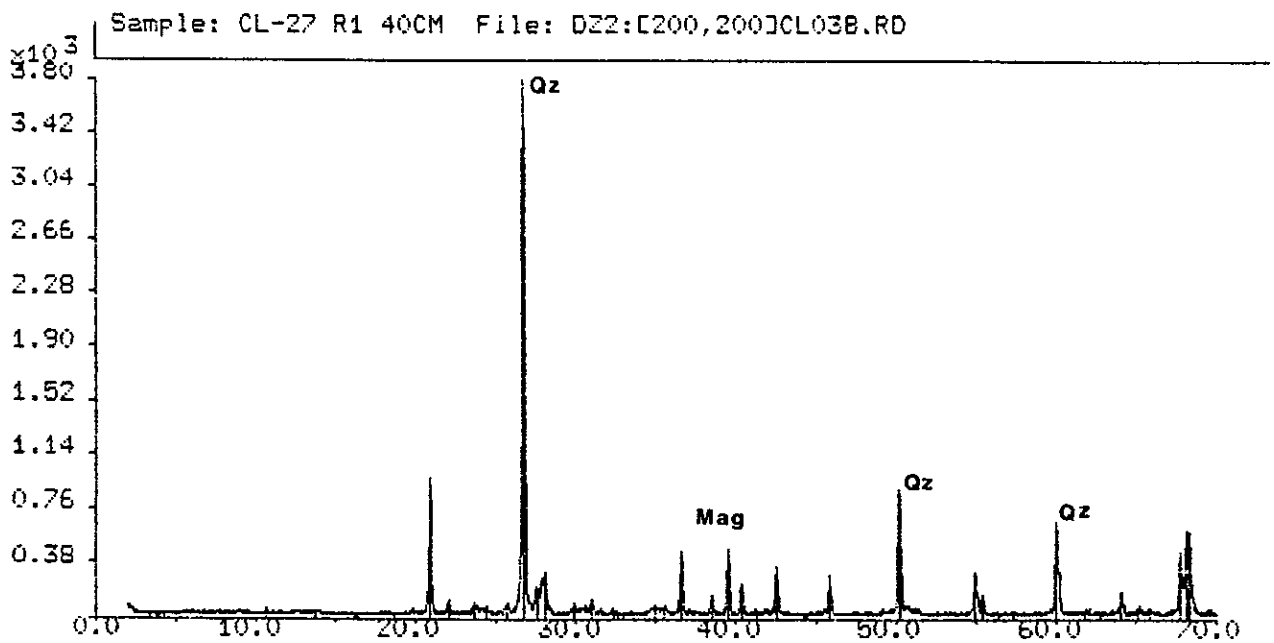

Figure 12. Mass spectrometer analysis of vibracore CI-87-27, Run 1 at 0.4 meters subbottom. See Figure 2 for location of vibracore, and Appendix 1-A for mineralogic analysis of sample.

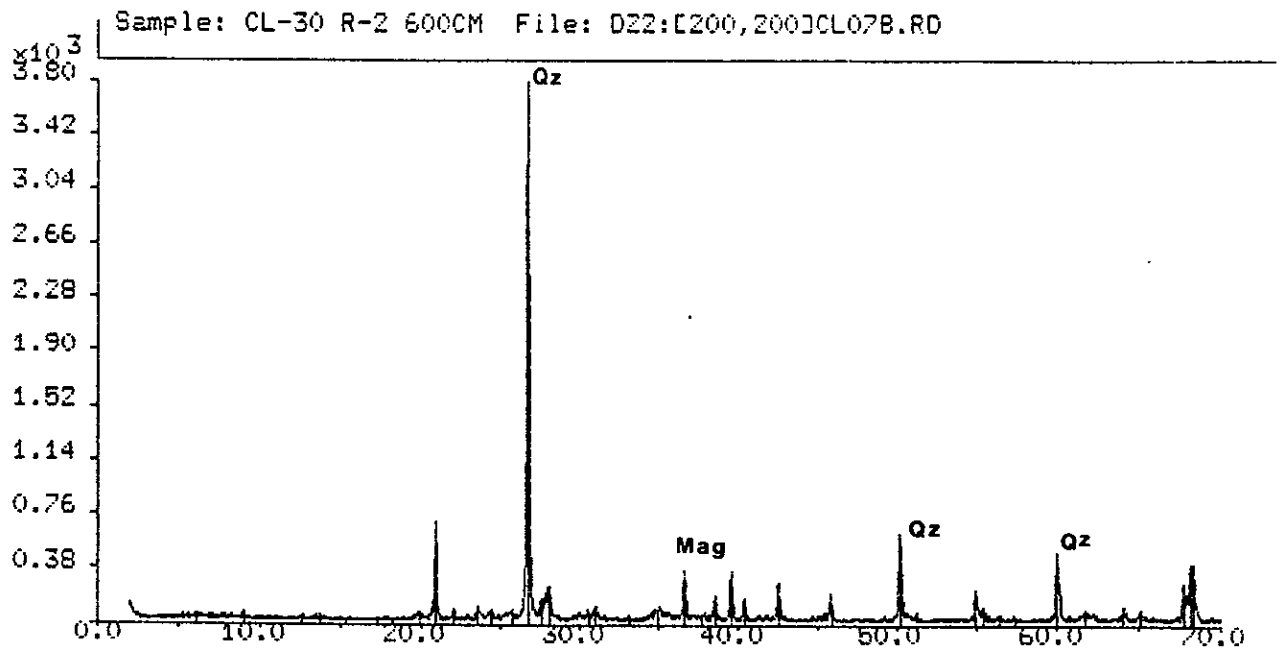

Figure 13. Mass spectrometer analysis of vibracore CI-87-30, Run 2 at 6.0 meters subbottom. See Figure 2 for location of vibracore, and Appendix 1-A for mineralogic analysis of sample.

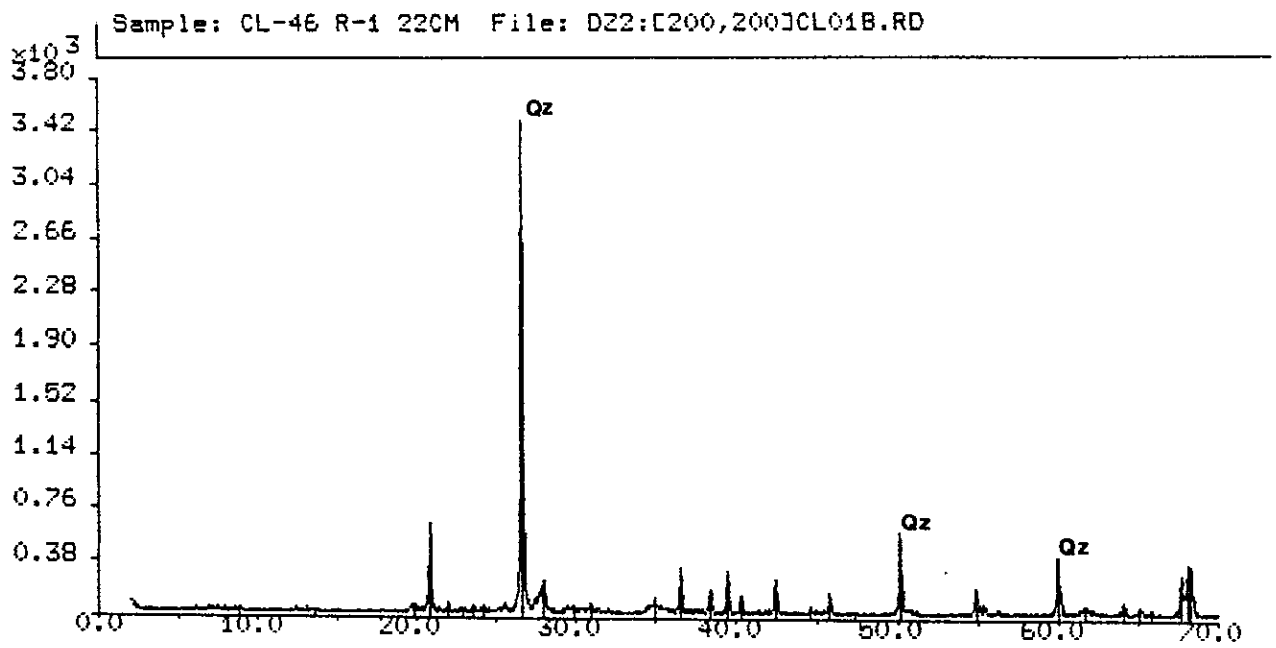

Figure 14. Mass spectrometer analysis of vibracore CI-87-46, Run 1 at 0.2 meters subbottom. See Figure 2 for location of vibracore, and Appendix 1-A for mineralogic analysis of sample.

to the NW (landward). The shoals are typically irregular to elongated in plan view and vary from less than 1 km^2 to over 25 km^2 in areal extent. The larger shoals are 5 to 8 km in length and 2 to 4 km in width (Penland et al. 1989). Spacing between sand shoals within the large shoal field is usually on the order of 1 km (Figure 15).

The shoals appear to migrate landward (NW) with the dominant wave approach over the seafloor by erosion of the leeward shoal face with deposition on the shoal crest and back shoal, similar to other shelf sand bodies formed on the U.S. Atlantic shelf (Boczar-Karakiewicz and Bona 1986; Duane et al. 1972; Figueirido 1984). Erosional scour associated with wave and current action is observed on seismic profiles between the larger shoals (Penland et al. 1989). Sand waves are also observed on the crests of individual shoals on side-scan sonographs, indicating the shoals are currently migrating in a landward direction (Figure 19). These inter-shoal areas are characterized by darker "mottled" gray tones on the sonographs, whereas the crests of the shoals have lighter uniform gray tones. The mottled inter-shoal areas consist predomininantly of muddy sand and silty sand, whereas the shoals are composed of fine-grained well sorted sand deposits.

Two main sets of shoal fields were mapped within the region, with the overall shoal trend striking NE/SW, oblique to the dominant direction of wave approach from the SE (Penland et al. 1989). The largest shoal trend lies in 20 to 26 m of water, with a minor shoal trend lying in about 15 m of water approximately 5 km landward (NW) of the larger shoal trend. The majority of sand shoals are oriented perpendicular (elongate) to the dominant direction of wave approach. However, three of the larger shoals are elongated NW/SE, parallel to the direction of dominant wave approach from the SE. The geometry of these shoals are believed to be related to their original source as distributary channel mouth bar deposits that were subsequently reworked into

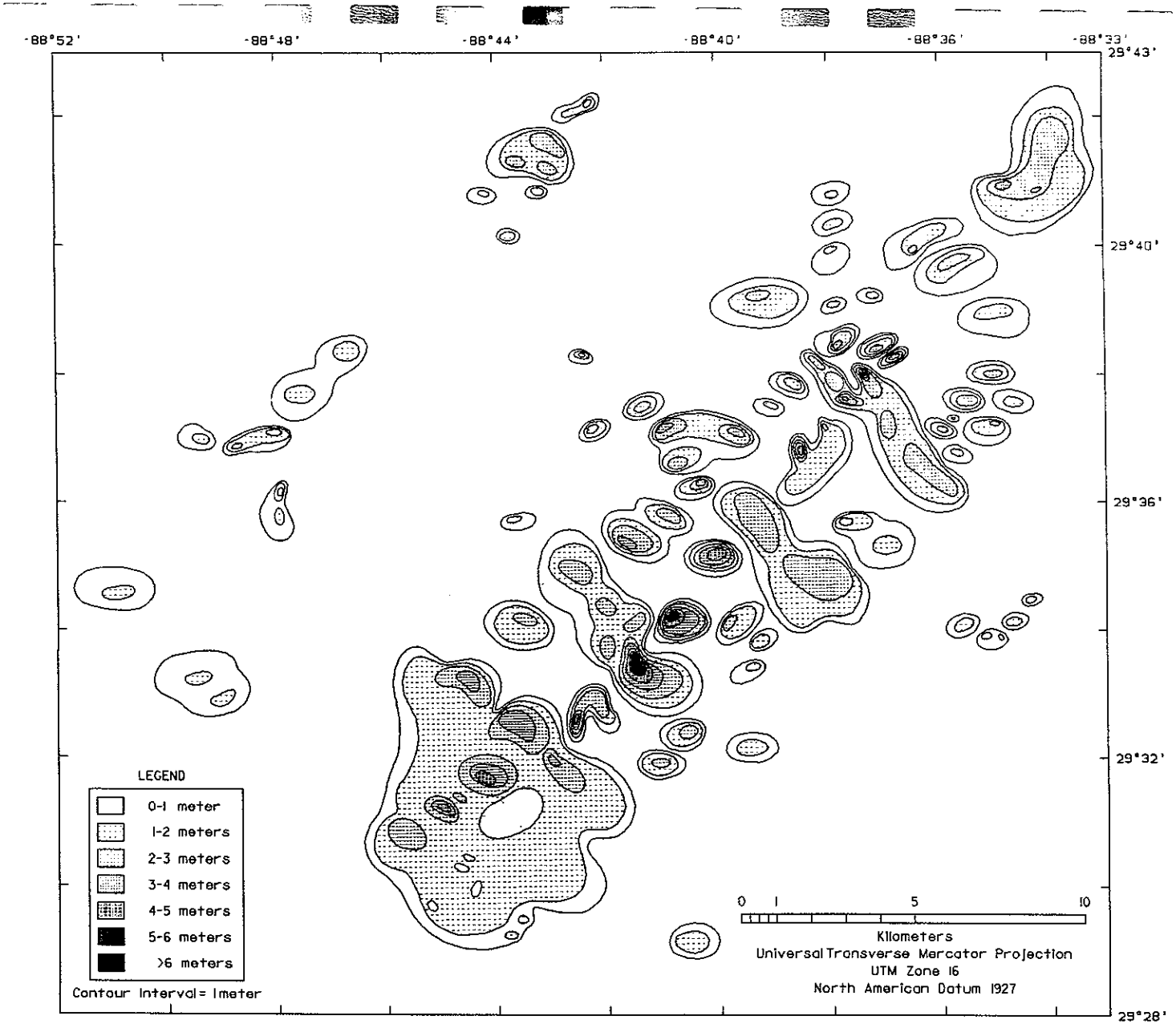

Figure 15. Isopach map of the St. Bernard Shoals. Note two major parallel shoal trends extending NE/SW. See Appendix 1-B for volumetric calculations of each sand shoal. Contour interval is 1 m.

tidal inlet sequences (i.e., washover, tidal channel, spit, flood- and ebb-tidal deltas). The orientation and geometry of smaller shoals flanking these linear sand bodies resemble sub-deltas (bay fills or crevasse splays) that formed from breaching of the main distributary channel during flooding, similar to those formed today in the lower Mississippi River delta (Coleman 1976; 1988).

Superimposed on the greater shoal trend is a set of 5 to 6 smaller sand ridges that form thicker sand accumulations on individual shoals, trending subparallel with the strike of the shoal trend (parallel to the direction of dominant wave approach). The geometry, morphology, and distribution of these shoal sand bodies demonstrate the importance of the orientation of the old deltaic headland to the dominant direction of wave approach, and their relationship to the distributary channel mouth bar and tidal inlet sequences as sediment sources (Penland et al. 1988; Kindinger 1988).

ST. BERNARD SHOALS GEOLOGY

Surficial sediment obtained from grab samples and vibracores consist of fine-grained well sorted quartzose sand of late Pleistocene to early Holocene age, and Recent sand, silt, and clay deposits distributed by the St. Bernard and Mississippi River deltas (Frazier 1974; Mazullo and Bates 1985; Kindinger 1988). Ludwick (1964) determined the shoals are composed of fine-grained (0.11 mm), well sorted (1.15 sorting coefficient) sand with modal characteristics of 94% terrigenous sand and 6% carbonate sand. Frazier (1974) and Kindinger et al. (1982) mapped similar surface distribution patterns of 75 to 100% fine-grained sand, with a sand sheet spreading seaward of the larger shoal sand body.

Depositional Environments

Six distinct depositional environments were interpreted through integrated analyses of vibracores and seismic profiles. Grain-size statistics, sedimentary texture, primary and secondary

physical structures, and sequence associations were used to characterize depositional environments and sedimentary facies. The regressive sedimentary environments were interpreted to include: (1) prodelta; (2) delta fringe; and (3) distributary channel. The transgressive sedimentary environments were interpreted to include: (1) lagoon; (2) barrier; and (3) shoal.

The prodelta environment was interpreted from core analysis as fine-grained laminated clay and silty clay deposits that form the platform upon which the distributary network prograded. The delta fringe environment consists of a coarsening-upward sequence of lenticular to wavy cross-beds of silt and sand interbedded with clay deposits. Distributary channel deposits are composed of channel fill and levee/overbank sand and silt, as well as the fine-grained fill that seals the channel.

The lagoon environment is composed of a coarsening-upward sequence of relatively thin interbedded mud with silt and thin (3 - 10 cm) sand storm beds or washover deposits. Primary physical structures include small to large burrows, wavy and lenticular silt and sand beds, and shell fragments. The typical barrier sequence coarsens-upward, and represents the transgressive contact between the muddy lagoon deposits and sand-prone flood-tidal delta and washover deposits. The barrier environment consists of recurved spits, tidal inlets, washover, ebb- and flood-tidal deltas, and sand sheet environments of deposition.

The shoal environment is massive in appearance, and is composed of a marine sand body derived from the reworking of the underlying barrier facies. The sand shoals are characterized by faint horizontal and planar bedding, mud-filled burrows, and shell fragments throughout. The typical shoal sequence coarsens upward, and is predominantly fine-grained clastic sand. The grain-size distribution of the shoal exceeds 92% sand, contains 6% silt, and usually exhibits less then 2% clay. The sands are characteristically rounded to subrounded and well to very well sorted.

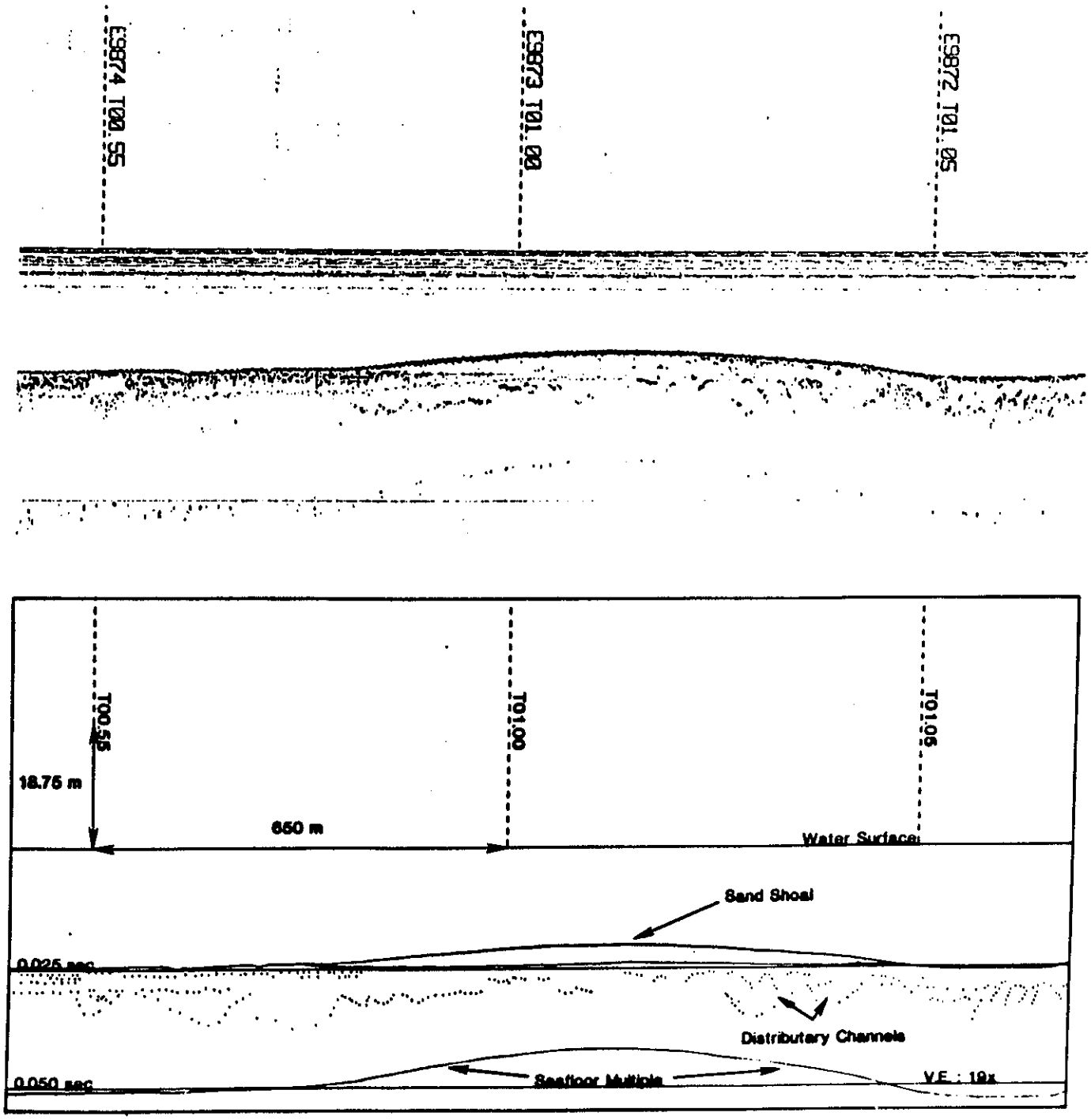

Figure 16. Uninterpreted 3.5-kHz subbottom profile and line drawing of a sand shoal. Seismic profile acquired during CCEER/USGS 1989 Acadiana survey. See Figure 2 for location of profile.

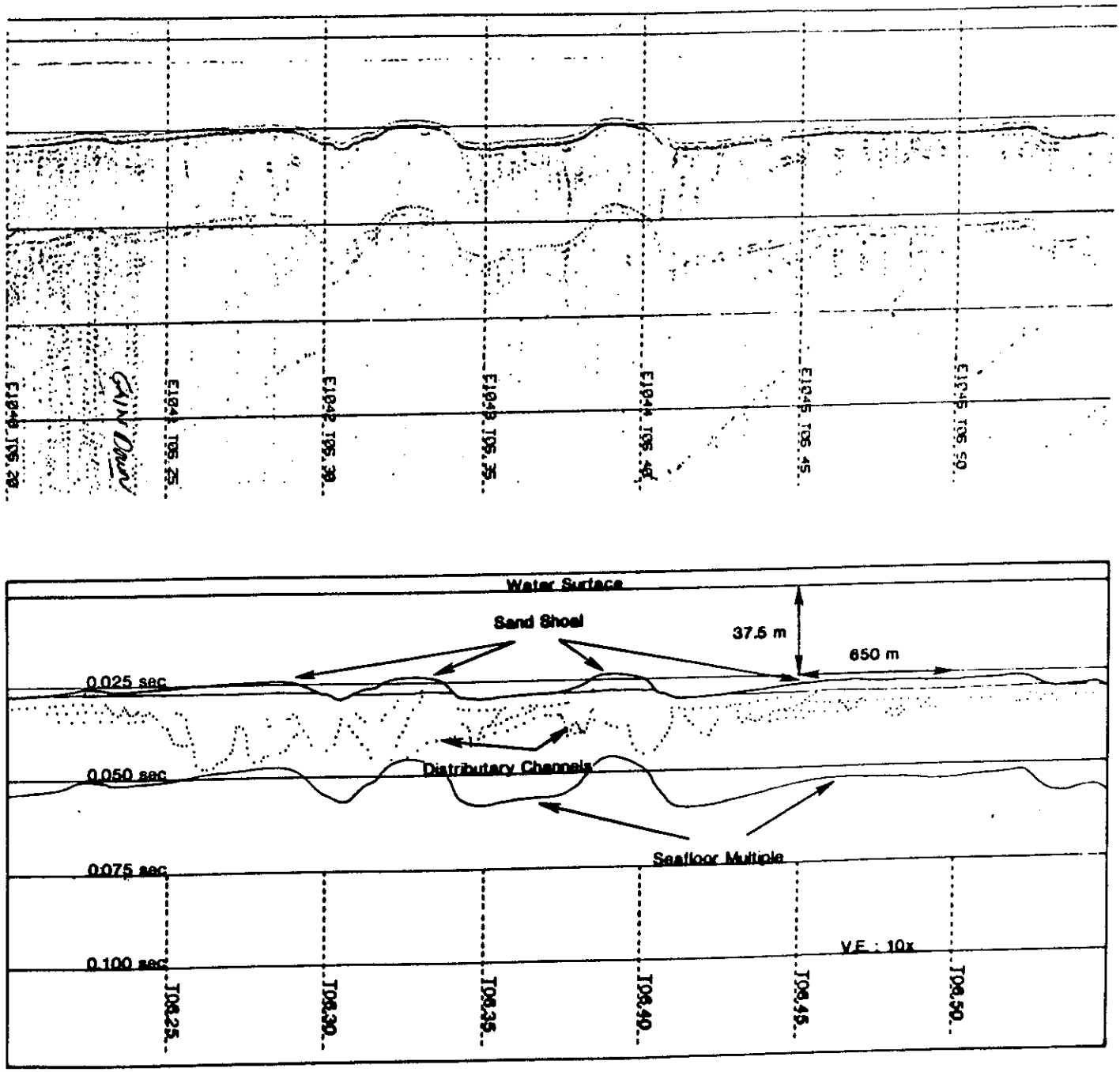

Figure 17. Uninterpreted ORE geopulse boomer record and line drawing of a sand shoal. Seismic profile acquired during CCEER/USGS 1987 Acadiana survey. See Figure 2 for location of profile.

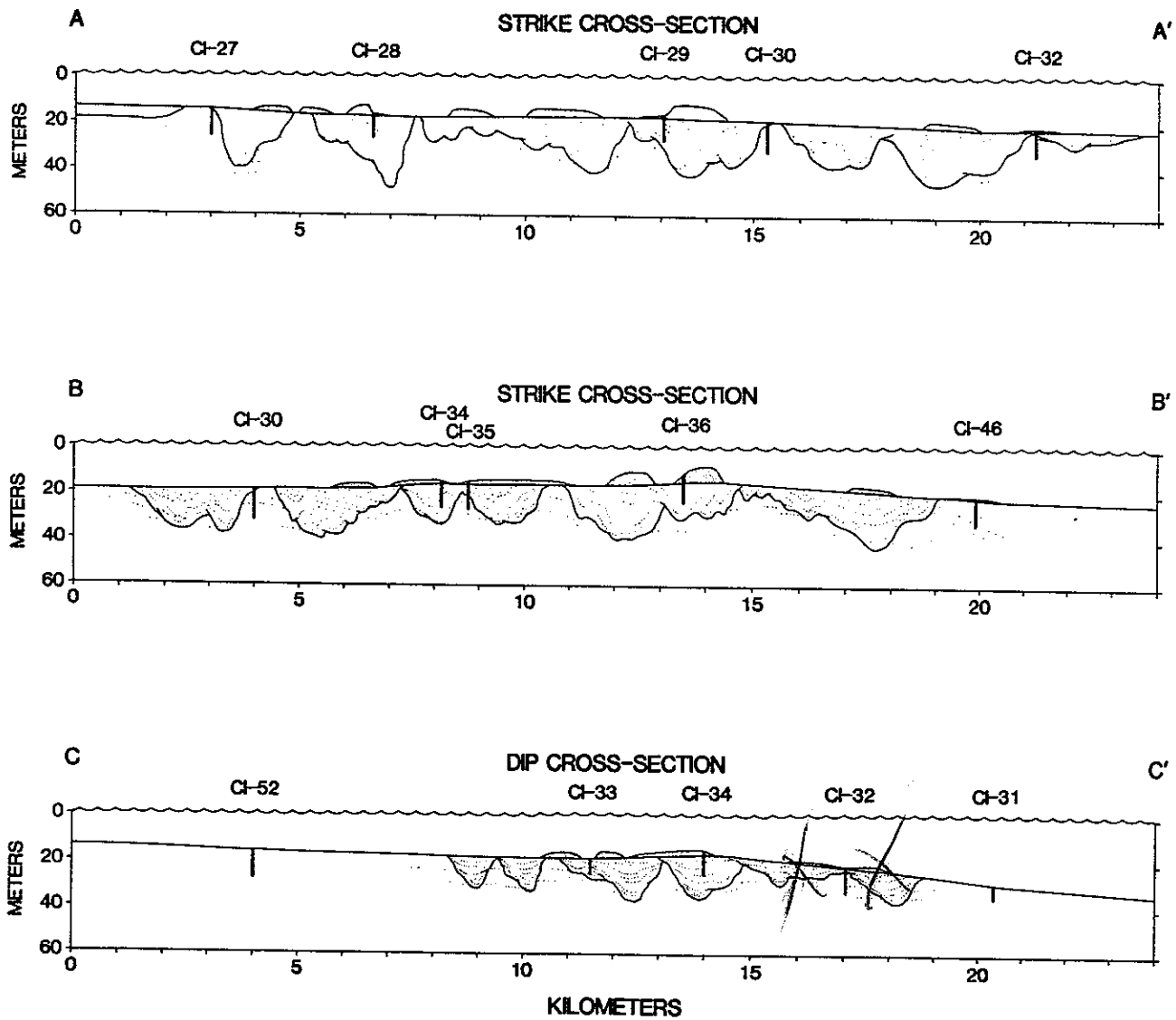

Figure 18. Schematic geologic cross sections A - A', B - B', and C - C'. Note flat bases of individual shoals, and their relationship to underlying distributary and/or tidal inlet systems. See Figure 20 for location of cross sections.

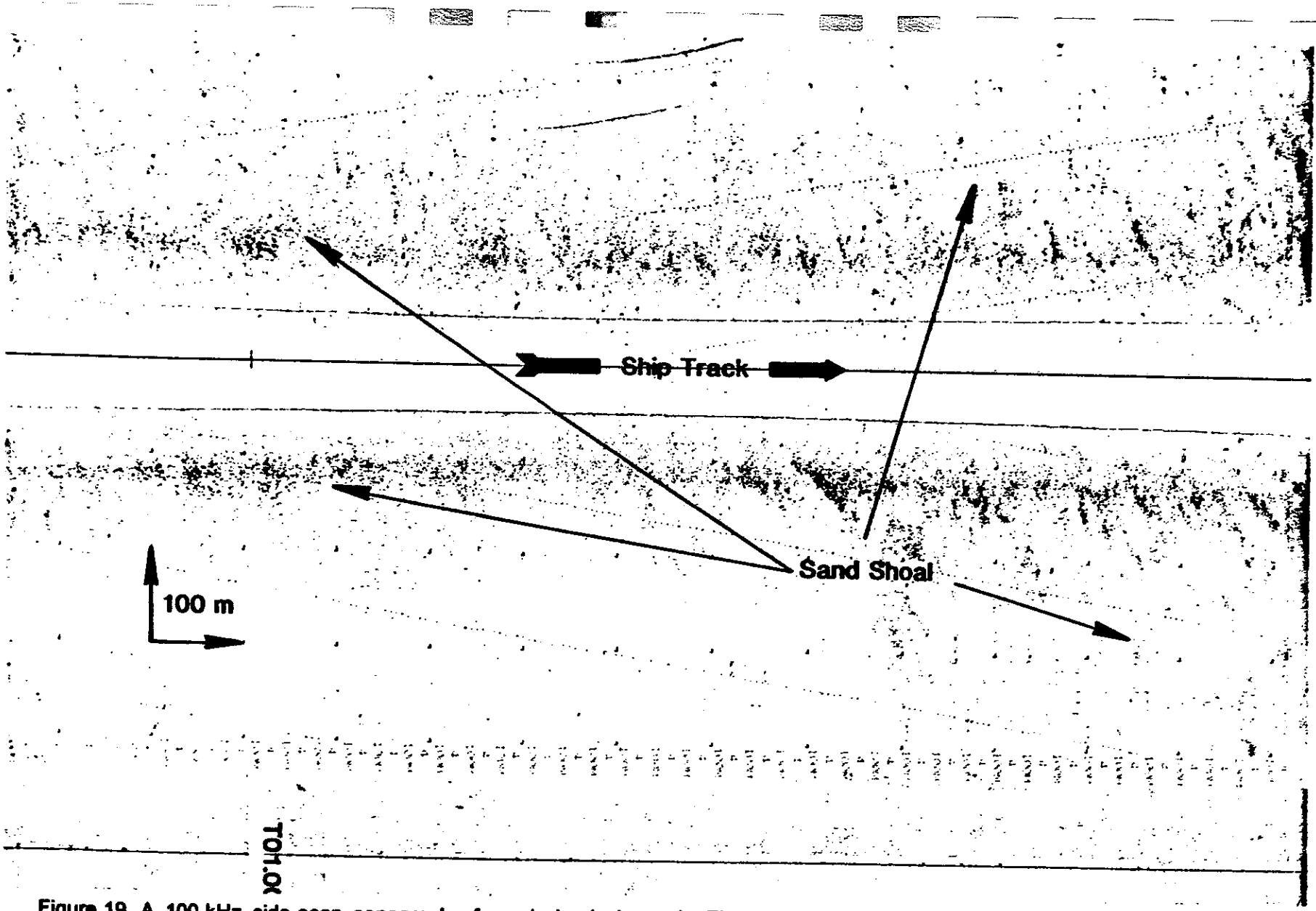

Figure 19. A 100-kHz side-scan sonograph of sand shoal shown in Figure 8. Sonograph acquired during CCEER/USGS 1989 Acadiana survey.

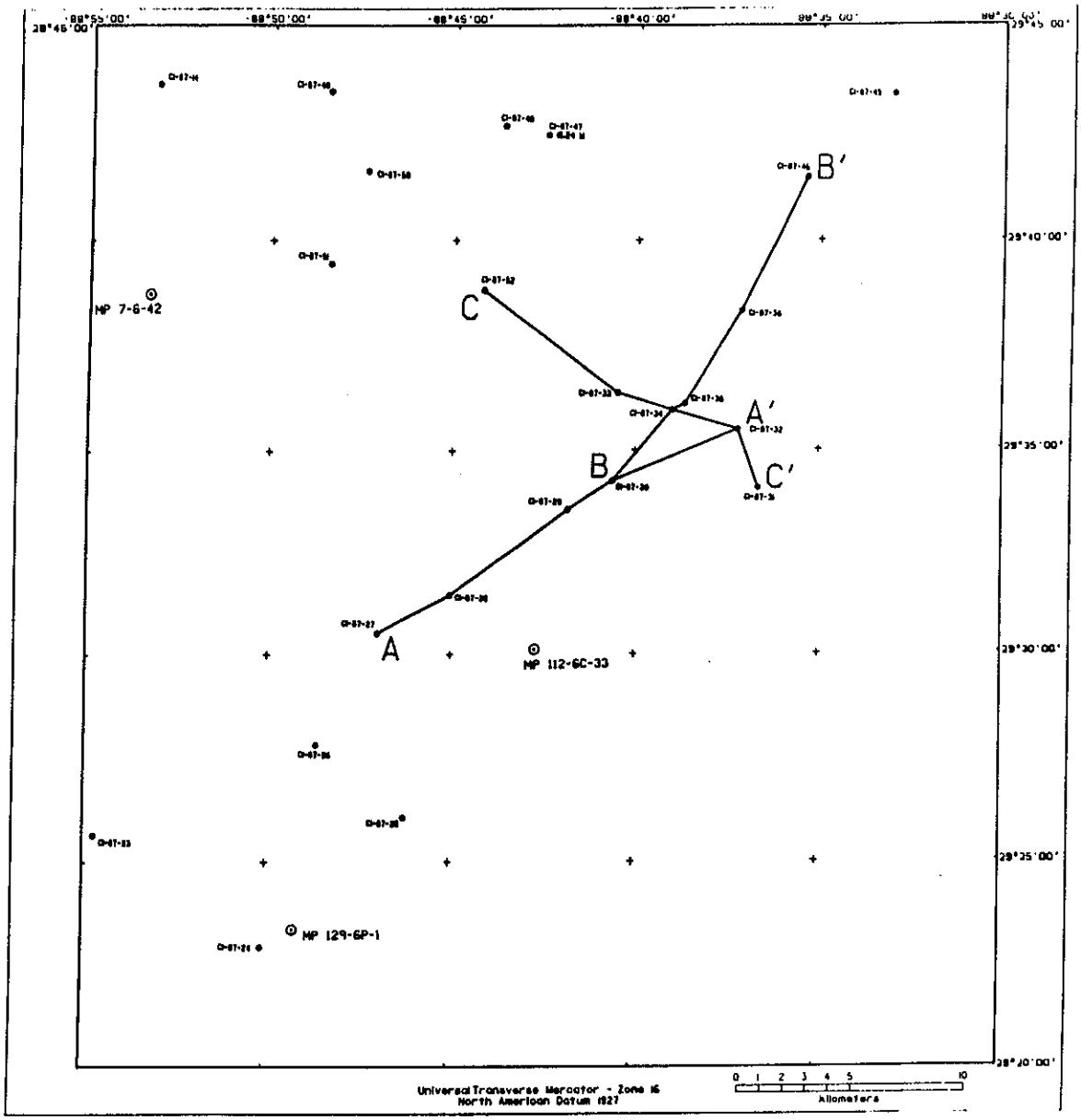

Figure 20. Location of geologic cross sections A - A', B - B', and C - C'.

Geologic Cross Sections

Seismic profiles, side-scan sonographs, and vibracore logs were integrated to construct two strike and one dip schematic cross sections (Figure 18 and 20). The schematic geologic cross sections shown in Figure 18 illustrate the interpreted depositional environments and facies associations. As noted previously, the major sand shoal bodies are observed to lie above the barrier (i.e., tidal inlet, ebb- and flood-tidal deltas, etc.) and/or distributary channel environments. The shoals are flat-based sand deposits that occur as isolated deposits in two separate NE/SW trends as described in detail earlier. The cross sections also illustrate the relationship of the major shoal trend to a subtle increase in seafloor slope seaward of the shoals.

Isopach Mapping

The St. Bernard Shoals isopach map was made through integration of seismic profiles and vibracore logs. Seismic profiles were calibrated to the sand shoal environment interpreted from the vibracore logs (Figure 3 - 7 and 17). The seismic character of the sand shoals was then used to map the distribution, orientation, geometry, trend, and thickness patterns of the shoals throughout the area (Figure 15). Approximate sand volumes contained within each shoal are tabulated in Appendix 1-B. The mineralogic analyses by mass spectrometer of seven sediment samples obtained from six of the vibracores are shown in Figures 8 through 14 and Appendix 1-A. Analysis of vibracores and high-resolution seismic profiles shows that the shoal sand bodies range in thickness from 1 to 6 m, and average 2 to 4 m in thickness (Figures 16 - 18). Calculated shoal volumes for the 61 individual sand shoals vary from 37,500 m^3 to almost 75.6 million m^3 for the largest shoal sand body (Appendix 1-B).

SUMMARY AND CONCLUSIONS

The St. Bernard Shoals vary considerably in morphology and geometry from the other shoals formed on the Louisiana continental shelf, such as Trinity Shoal and Ship Shoal. These shoals are submerged barrier islands, and consist primarily of one continuous sand body whose sedimentary (sand-prone) facies are buried in the subsurface. In contrast, the St. Bernard Shoals are flat-based and isolated undulating mound features that lie directly on the seafloor above channel-fill facies.

The difference in morphology and geometry of these shoals may be attributed to a higher sediment accumulation rate that allowed the St. Bernard delta to prograde into deeper water than the Teche and Maringouin deltas whose deposits were reworked into Trinity Shoal and Ship Shoal. During the destructional phase of the delta cycle, the St. Bernard distributary mouth bar and tidal inlet sequences may therefore have undergone a faster rate of transgressive submergence than the Teche and Maringouin deltas formed on the central Louisiana continental shelf.

Transgression of the barrier due to delta abandonment and relative sea level rise often generates a new shoreline farther landward. The barrier and lagoonal deposits that formed after the abandonment of the St. Bernard delta were probably only slightly reworked and only partially drowned in-situ. This may account for the minor shoal trend observed about 5 km landward of the larger shoal trend which marks the location of the subsequent shoreline. These processes may account for isolated shoals similar in morphology to the Chandeleur Islands, rather than a single, reworked barrier island sand body.

The transgressive submergence model described by Penland et al. (1988) may best explain the origin, morphology, and geometry of the St. Bernard Shoals. This model describes a process whereby the morphology and stratigraphy of each transgressive depositional system

reflects its position in an evolutionary 3-stage sequence. This sequence begins after delta abandonment, when marine processes transform the abandoned deltaic complex into stage 1, an erosional headland with flanking barrier islands. Relative sea level rise, subsidence, land loss, and shoreface erosion lead to submergence and separation of the stage 1 barrier shoreline from the mainland described by Hoyt (1967), forming stage 2, the barrier island arc. Submergence of the barrier island arc eventually occurs due to its inability to keep pace with relative sea level rise, ongoing subsidence, and overwash processes. The stability threshold of the island arc is exceeded and the subaerial integrity depleted leading way for subaqueous environments to evolve. This process initiates stage 3, an inner-shelf shoal. Following submergence, marine processes continue to rework the inner-shelf shoal into a marine sand body on the shoreface and inner continental shelf.

The St. Bernard Shoals contain almost 200 million m^3 of sand that could be used for shoreline erosion control. The shoal's transgressive sand facies offer the best source of material for coastal erosion control projects in terms of volume and quality. Additional sand resources are also available in the subsurface in the form of tidal inlet sequences and channel fill facies as interpreted from seismic profiles. Further acquisition of side-scan sonographs that allow construction of mosaics throughout the major shoal field will enable the true areal extent, geometry, and total volume of quality sand contained within the St. Bernard Shoals to be more accurately determined.

REFERENCES CITED

Barth, M.C., and Titus, J.G., 1984, Greenhouse Effect and Sea Level Rise: New York, Van Nostrand Reinhold Co., 325 p.

Boczar-Karakiewicz, B., and Bona, J.L., 1986, Wave-dominated shelves: a model of sand ridge formation by progressive, infragravity waves, *in* Knight, R.J., and McLeon, J.R., eds., Shelf Sands and Sandstones, Can. Soc. Pet. Geol. Mem. 11, p. 163-179.

Britsch, L.D., and Kemp, E.B., III, 1990, Land loss rates: Mississippi River deltaic plain: New Orleans, Technical Report GL-90-02, U.S. Army Corps of Engineers, 35 p.

Bruun, P., 1988, Rationalities of coastal erosion and protection: An example from the Hilton Head Island, South Carolina: Jour. Coastal Research, v.4, no. 1, p. 129-138.

Bruun, P., 1988a, Profile nourishment: Its background and economic advantages: Jour. Coastal Research, v. 4, no. 2, p. 219-228.

Byrnes, M.R., Penland, P., Ramsey, K.E., Crawford, T.G., Kelly, R.F., and Rowland J., 1991, Offshore sand resources for coastal erosion control in Louisiana: Physical environmental considerations and economic feasibility. In MTS '91 Proceedings, Marine Technology Society, Washington, DC, p. 755-761.

Byrnes, M.R., and Patnaik, P. 1991, An evaluation of the physical environmental impacts of sand dredging on Ship Shoal. In : Byrnes, M.R., and Groat, C. G., eds., Characterization of the Development Potential of Ship Shoal Sand for Beach Replenishment of the Isles Dernieres. Final Report to U.S. Minerals Management Service, Cooperative Agreement #14-21-0001-30404, p. 83-130.

Coleman, J.M., 1976, Deltas - Processes of Deposition and Models for Exploration: Champaign: Continuing Education Pub. Co., 102 p.

Coleman, J.M., 1988, Dynamic changes and processes in the Mississippi River delta: Geol. Soc. America Bull., v. 100, p. 999-1015.

Coleman, J.M., and Gagliano, S.M., 1964, Cyclic sedimentation in the Mississippi River deltaic plain: Trans. Gulf Coast Assoc. Geological Societies, v. 14, p. 67-82.

Coleman, J.M., Prior, D.B., and Lindsay, J.F., 1983, Deltaic influences on shelf edge instability processes, *in* Stanley, D.J., and Moore, G.T., eds., The Shelf Break: Critical Influence on Continental Margins: Soc. Econ. Paleontologists Mineralogists Spec. Pub. 33, p. 121-137.

Coleman, J.M., and Roberts, H.H., 1988, Sedimentary development of the Louisiana continental shelf related to sea level cycles: Part I--sedimentary sequences: Geo-Marine Letters, v. 8, no. 2, p. 63-108.

Coleman, J.M., and Roberts, 1988a, Sedimentary development of the Louisiana continental shelf related to sea level cycles: Part II--seismic response: Geo-Marine Letters, v. 8, no. 2, p. 109-119.

Coleman, J.M., and Roberts, H.H., 1991, Coastal Depositional Systems in the Northern Gulf of Mexico, *in* Perkins, R.F., ed., Coastal Depositional Systems in the Northern Gulf of Mexico: Quaternary Framework and Environmental Issues: Gulf Coast Sec. Soc. Econ. Paleontologists Mineralogists Foundation Twelfth Annual Research Conf., p. 62-64.

Craig, N.J., Turner, R.E., and Day, J.W., Jr., 1980, Wetland loss and their consequences in coastal Louisiana: Z. Geomorph. N.F., Suppl. Bull. 34, p. 225-241.

Curray, J.R., 1960, Sediments and history of Holocene transgression, continental shelf, northwest Gulf of Mexico, *in* Shepard, F.P., Phleger, F.B., and van Andel, T.H., eds., Recent Sediments, Northwest Gulf of Mexico: Am. Assoc. Petroleum Geologists, p. 221-266.

Dolan, R., Anders, F., and Kimball, S., 1985, Map of coastal erosion and accretion, *in* National Atlas of the U.S.A.: Reston, U.S. Department of the Interior, U.S. Geological Survey, Scale 1:7,500,000.

Duane, D.B., Field, M.E., Meisburger, E.P., Swift, D.J.P., and Williams, S.J., 1972, Linear shoals on the Atlantic inner continental shelf, Florida to Long Island, *in* Swift, D.J.P., Duane, D.B., and Pilkey, O.H., eds., Shelf Sediment Transport: Process and Pattern: Stroudsburg: Dowden, Hutchinson, and Ross, p. 447-498.

Dunbar, J.B., Britsch, L.D., and Kemp, E.B., III, 1990, Land loss rates: Louisiana Chenier Plain: Vicksburg: Technical Report No. 2, GI-90-2, U.S. Army Corps of Engineers, Waterways Experiment Station, 21 p.

Fisk, H.N., 1944, Geologic investigation of the alluvial valley of the lower Mississippi River: Vicksburg, U.S. Army Corps of Engineers Mississippi River Commission, 78 p.

Figueiredo, A.G., 1984, Submarine sand ridges: geology and development, New Jersey, U.S.A. [Unpublished Ph.D. Dissertation]: Coral Gables, University of Miami, 385 p.

Frazier, D.E., 1967, Recent deposits of the Mississippi River, their development and chronology: Trans. Gulf Coast Assoc. Geological Societies, v. 17, p. 287-311.

Frazier, D.E., 1974, Depositional episodes: their relationship to the Quaternary stratigraphic framework in the northwestern portion of the Gulf Basin: Austin, Texas Bureau of Economic Geology Circular 74-1, 28 p.

Jones, R.S., and Edmonson, J.B., 1987, The Isles Dernieres barrier island shoreline restoration project, *in* Penland, S., and Suter, J.R., eds., Barrier Shoreline Geology, Erosion, and Protection in Louisiana: Coastal Sediments '87 Field Guide: Am. Soc. Civil Engineers, p. 5-1--5-5.

Kindinger, J.L., Miller, J.R., Stelting, C.E., and Bouma, A.H., 1982, Depositional history of the Louisiana-Mississippi outer continental shelf: Reston, U.S. Geological Survey Open-File Report 82-1077, 55 p.

Kindinger, J.L., 1988, Seismic stratigraphy of the Mississippi-Alabama shelf and upper continental slope: Marine Geology, v. 83, p. 79-94.

Kolb, C.R., and Van Lopik, J.R., 1958, Geology of the Mississippi River deltaic plain, southeastern Louisiana: Vicksburg, Report 3-483, U.S. Army Corps of Engineers, Waterways Experiment Station, 120 p.

Krawiec, W., 1966, Recent Sediments of the Louisiana Inner Continental Shelf [Unpublished Ph.D. Dissertation]: Houston, Rice University, 50 p.

Ludwick, J.C., 1964, Sediments in the northeastern Gulf of Mexico, *in* Miller, R.L., ed., Papers in Marine Geology, Shepard Commemorative Volume, New York, MacMillan, p. 204-238.

May, J.P., 1974, WAVENRG: A computer program to determine the distribution of energy dissipation in shoaling water waves, with examples from coastal Florida, *in* Tanner, W.F., ed., Sediment Transport in the Nearshore Zone, Tallahassee, Florida State University, p. 22-80.

Mazullo, J., and Bates, C., 1985, Sources of Pleistocene and Holocene sand for the northeast Gulf of Mexico shelf and Mississippi Fan: Trans. Gulf Coast Assoc. Geological Societies, v. 35, p. 457-466.

Mitchum, R.M., Jr., Vail, P.R., and Sangree, J.B., 1977, Stratigraphic interpretation of seismic reflection patterns in depositional sequences, *in* Payton, C.E., ed., Seismic Stratigraphy--Applications to Hydrocarbon Exploration, Am. Assoc. Petroleum Geology Memoir 26, p. 117-134.

Mossa, J., 1988, Analysis of the environmental effects of sand resource utilization on the Louisiana continental shelf: Baton Rouge, Louisiana Geological Survey Open-File Series No. 88-01, 31 p.

National Research Council, 1987, Responding to Changes in Sea Level: Washington, D.C., National Academy Press, 148 p.

Penland, S., and Suter, J.R., 1988, Barrier island erosion and protection in Louisiana: A coastal geomorphological perspective: Trans. Gulf Coast Assoc. Geological Societies, v. 38, p. 331-342.

Penland, S., Boyd, R., and Suter, J.R., 1988, The transgressive depositional systems of the Mississippi River delta plain: a model for barrier shoreline and shelf sand development: Jour. Sed. Petrology, v. 58, no. 6, p. 932-949.

Penland, S., Suter, J.R., McBride, R.A., Williams, S.J., Kindinger, J.L., and Boyd, R., 1989, Holocene sand shoals offshore of the Mississippi River delta plain: Trans. Gulf Coast Assoc. Geological Societies, v. 39, p. 471-480.

Penland, S., and Ramsey, K.E., 1990, Relative sea level rise in Louisiana and the Gulf of Mexico: 1908-1988: Jour. Coastal Research, v. 6, no. 2, p. 323-342.

Penland, S., Roberts, H.H., Williams, S.J., Sallenger, A.H., Cahoon, D.R., Davis, D.W., and Groat, C.G., 1990, Coastal land loss in Louisiana: Trans. Gulf Coast Assoc. Geological Societies, v. 40, p. 685-699.

Penland, S., Suter, J.R., Ramsey, K.E., McBride, R.A., Williams, S.J., and Groat, C.G., 1990a, Offshore sand resources for coastal erosion control in Louisiana: Trans. Gulf Coast Assoc. Geological Societies, v. 40, p. 721-731.

Penland, S., McBride, R.A., Suter, J.R., Boyd, R., and Williams, S.J., 1991, Holocene development of shelf-phase Mississippi River delta plains, *in* Perkins, B.F., ed., Coastal Depositional Systems in the Gulf of Mexico: Quaternary Framework and Environmental Issues: GCSSEPM Twelfth Annual Research Conference, p. 182-185.

Ramsey, K.E., Penland, S., and Roberts, H.H., 1991, Implications of accelerated sea level rise on Louisiana coastal environments: Proc. Coastal Sediments '91, Am. Soc. Civil Engineers, Water Resources Div., p. 1207-1222.

Suter, J.R., and Berryhill, H.L., Jr., 1985, Late Quaternary shelf margin deltas, northwest Gulf of Mexico: Am. Assoc. Petroleum Geologists, v. 69, no. 1, p. 77-91.

Suter, J.R., Berryhill, H.L., Jr., and Penland, S., 1987, Late Quaternary sea level fluctuations and depositional sequences, southwest Louisiana continental shelf, *in* Nummedal, D., Pilkey, O.H., and Howard, J.D., eds., Sea Level Fluctuation and Coastal Evolution: Soc. Economic Paleontologists Mineralogists Special Pub. 41, p. 199-219.

Suter, J.R., et al, 1989, Preliminary assessment of the occurrence and effects of utilization of sand and aggregate resources on the Louisiana inner shelf: Marine Geology, v. 90, p. 31-37.

Suter, J.R., Boyd, R., and Penland, S., 1991, Late Quaternary chronostratigraphic framework, northern Gulf of Mexico, *in* Perkins, B.F., ed., Coastal Depositional Systems in the Gulf of Mexico: Quaternary Framework and Environmental Issues, Twelfth Annual Research Conference, GCS/SEPM, p. 263-264.

Titus, J.G., ed., 1987, Greenhouse Effect, Sea Level Rise and Coastal Wetlands: Washington, D.C., Environmental Protection Agency, Office of Wetland Protection, 152 p.

van Beeck, J.L., and Meyer-Arendt, K.J., 1982, Louisiana's eroding coastline: recommendations for protection: Baton Rouge, Louisiana Department of Natural Resources, 49 p.

APPENDIX 1-A
Mass Spectrometer Data Sheets

APD 3720 @ LSU Geology Department (DETECTED MASS SPECTROMETER PEAKS)

Listed DI file name	:	DZ2:[200.200]CLO4B.DI
Raw data file name	:	DU:CLO6B.RD;00001
Sample identification	:	*CL-24 RI 220CM*
Measurement date/time	:	5-DEC-90 8:50
Generator settings	:	40 kV, 21 mA
Cu alpha1,2 wavelengths	:	1.54060, 1.54439 ang
Step size, sample time	:	0.040 deg, 1.00 s, 25.00 s/deg
Monochromator used	:	YES
Divergence slit	:	Automatic (Specimen length: 13.0 mm)
Analysis program number	:	2
Peak angle range	:	2.000 - 70.000 deg
Range in D spacing	:	1.34298 - 44.1372 ang
Peak position criterion	:	Top of smoothed data
Cryst peak width range	:	0.00 - 2.00 deg
Minim peak significance	:	0.75
Number of peaks in file	:	37 (Alpha1: 33, Amorphous: 0)
Maximum Intensity	:	5141. cts, 5140.9 cps

Peak (no)	Angle (deg)	Tip width (deg)	Peak (cts)	Back g (cts)	D spac (ang)	I/Imax (%)	Type (A1 A2 Ot)	Sign
1	8.3700	1.60	10.	38.	10.5554	0.20	X X	0.76
2	13.6075	0.64	19.	34.	6.5021	0.38	X X	0.85
3	19.7500	0.20	31.	29.	4.4916	0.61	X X	0.87
4	20.9025	0.12	841.	29.	4.2464	16.36	X X	4.47
5	22.0400	0.16	114.	30.	4.0298	2.23	X X	2.24
6	23.6625	0.20	77.	30.	3.7570	1.51	X X	1.91
7	24.3200	0.32	53.	31.	3.3047	1.04	Bt	1.26
8	25.6700	0.24	77.	31.	3.4676	1.51	X X	1.78
9	26.6825	0.16	5141.	31.	3.3382	100.00	X X	24.55
10	28.0050	0.16	259.	32.	3.1835	5.04	X X	2.14
11	29.8800	0.24	50.	32.	2.9879	0.98	X X	1.26
12	30.9825	0.28	104.	34.	2.8840	2.02	X X	4.27
13	32.4550	0.24	15.	34.	2.7565	0.30	X X	0.81
14	35.0125	0.32	56.	35.	2.5608	1.09	X X	0.81
15	36.5975	0.16	441.	34.	2.4534	8.58	X X	5.13
16	38.4350	0.16	222.	34.	2.3402	4.32	X X	3.31
17	39.5175	0.16	412.	34.	2.2786	8.02	X X	5.27
18	40.3175	0.16	207.	34.	2.2352	4.03	X X	3.24
19	41.1525	0.24	24.	32.	2.1918	0.47	X X	0.95
20	42.4800	0.16	317.	32.	2.1263	6.16	X X	3.89
21	44.8825	0.48	28.	31.	2.0179	0.55	X X	1.35
22	45.8350	0.16	228.	31.	1.9781	4.44	X X	2.82
23	47.2125	0.48	13.	30.	1.9236	0.25	X X	0.95
24	48.3025	0.24	21.	30.	1.8827	0.41	X X	0.79
25	50.3025	0.24	773.	29.	1.8167	15.03	X X	13.18
26	50.7200	0.16	85.	29.	1.7985	1.65	X X	1.07
27	51.3775	0.40	40.	29.	1.7770	0.77	X X	1.05
28	54.8600	0.12	256.	37.	1.6721	4.98	X X	1.45
29	55.3450	0.16	102.	37.	1.6586	1.98	X X	1.20
30	57.2700	0.32	12.	36.	1.6074	0.22	X X	0.76
31	59.9375	0.12	552.	34.	1.5421	10.74	X	3.09
32	60.1600	0.08	237.	34.	1.5407	4.61	X	1.66
33	61.7725	0.48	25.	35.	1.5006	0.49	X X	1.05
34	64.0175	0.12	123.	36.	1.4533	2.40	X X	0.91
35	67.7000	0.12	380.	36.	1.3829	7.40	Ot	2.09
36	68.1200	0.08	480.	36.	1.3754	9.33	X	3.16
37	68.3200	0.08	475.	36.	1.3752	9.24	X	4.07

APD 3720 @ LSU Geology Department (DETECTED MASS SPECTROMETER PEAKS)

Listed DI file name	:	DZ2:[200.200]CLO6B.DI
Raw data file name	:	DU:CLO6B.RD;00002
Sample identification	:	*CL-24 RI 590CM*
Measurement date/time	:	6-DEC-90 12:01
Generator settings	:	40 kV, 21 mA
Cu alpha1,2 wavelengths	:	1.54060, 1.54439 ang
Step size, sample time	:	0.040 deg, 1.00 s, 25.00 s/deg
Monochromator used	:	YES
Divergence slit	:	Automatic (Specimen length: 13.0 mm)
Analysis program number	:	2
Peak angle range	:	2.000 - 70.000 deg
Range in D spacing	:	1.34298 - 44.1372 ang
Peak position criterion	:	Top of smoothed data
Cryst peak width range	:	0.00 - 2.00 deg
Minim peak significance	:	0.75
Number of peaks in file	:	36 (Alpha1: 32, Amorphous: 0)
Maximum intensity	:	4382. cts, 4382.4 cps

Peak (no)	Angle (deg)	Tip width (deg)	Peak (cts)	Back g (cts)	D spac (ang)	I/Imax (%)	Type (A1 A2 Ot)	Sign
1	13.7000	0.64	18.	30.	6.4584	0.40	X X	0.91
2	20.9800	0.12	660.	30.	4.2309	15.07	X X	4.17
3	22.1325	0.16	66.	30.	4.0132	1.50	X X	1.20
4	23.6975	0.16	81.	29.	3.7515	1.85	X X	1.07
5	24.3625	0.24	49.	29.	3.2990	1.12	Bt	0.81
6	25.7125	0.24	62.	28.	3.4619	1.42	X X	1.58
7	26.7600	0.16	4382.	28.	3.3287	100.00	X X	22.91
8	27.5350	0.20	128.	27.	3.2368	2.91	X X	1.62
9	28.0975	0.12	237.	27.	3.1733	5.41	X X	1.07
10	29.5750	0.20	36.	27.	3.0180	0.82	X X	1.05
11	29.9400	0.12	58.	26.	2.9820	1.32	X X	1.00
12	30.5875	0.12	53.	26.	2.9204	1.22	X X	0.81
13	31.3675	0.12	108.	26.	2.8763	2.47	X X	0.81
14	32.4875	0.32	17.	25.	2.7538	0.38	X X	0.79
15	35.6675	0.20	36.	36.	2.5152	0.82	X X	1.10
16	36.6425	0.16	396.	36.	2.4505	9.04	X X	5.62
17	38.5275	0.16	81.	34.	2.3348	1.85	X X	1.78
18	39.5600	0.16	346.	32.	2.2762	7.89	X X	5.13
19	40.40000	0.16	169.	32.	2.2308	3.86	X X	3.02
20	41.2750	0.16	35.	32.	2.1855	0.79	X X	0.81
21	42.5550	0.16	306.	31.	2.1227	6.99	X X	4.47
22	44.9425	0.32	18.	29.	2.0153	0.4	X X	0.83
23	45.8725	0.16	202.	29.	1.9766	4.60	X X	3.24
24	47.2200	0.48	10.	29.	1.9233	0.23	X X	0.98
25	50.2450	0.20	713.	28.	1.8144	16.27	X X	9.33
26	53.3275	0..24	24.	19.	1.7165	0.55	X X	0.87
27	54.9525	0.16	240.	21.	1.6696	5.48	X X	3.09
28	55.4175	0.16	110.	22.	1.6566	2.52	X X	1.45
29	60.0200	0.12	511.	30.	1.5401	11.65	X X	2.45
30	61.6975	0.64	21.	30.	1.5022	0.48	X X	0.79
31	64.0800	0.08	121.	30.	1.4520	2.76	Ot	2.95
32	65.1575	0.32	36.	31.	1.4306	0.82	X X	0.89
33	65.8275	0.12	36.	31.	1.4176	0.82	X X	0.79
34	67.7775	0.12	346.	32.	1.3815	7.89	Ot	2.00
35	68.2000	0.08	449.	34.	1.3740	10.26	X	3.02
36	68.4000	0.08	372.	34.	1.3738	8.50	X	2.82

APD 3720 @ LSU Geology Department (DETECTED MASS SPECTROMETER PEAKS)

Listed DI file name	:	DZ2:[200.200]CLO2B.DI
Raw data file name	:	DU:CLO2B.RD;00002
Sample identification	:	*CL-26 RI 40CM*
Measurement date/time	:	5-DEC-90 12:29
Generator settings	:	40 kV, 21 mA
Cu alpha1,2 wavelengths	:	1.54060, 1.54439 ang
Step size, sample time	:	0.040 deg, 1.00 s, 25.00 s/deg
Monochromator used	:	YES
Divergence slit	:	Automatic (Specimen length: 13.0 mm)
Analysis program number	:	2
Peak angle range	:	2.000 - 70.000 deg
Range in D spacing	:	1.34298 - 44.1372 ang
Peak position criterion	:	Top of smoothed data
Cryst peak width range	:	0.00 - 2.00 deg
Minim peak significance	:	0.75
Number of peaks in file	:	35 (Alpha1: 32, Amorphous: 0)
Maximum intensity	:	4396. cts, 4395.7 cps

Peak (no)	Angle (deg)	Tip width (deg)	Peak (cts)	Back g (cts)	D spac (ang)	I/Imax (%)	Type (A1 A2 Ot)	Sign
1	13.3950	0.96	12.	30.	6.6048	0.28	X X	1.32
2	19.7900	0.24	29.	25.	4.4826	0.66	X X	0.79
3	20.8825	0.16	708.	25.	4.2505	16.10	X X	9.55
4	22.0225	0.12	71.	26.	4.0329	1.61	X X	0.81
5	22.9950	0.24	26.	26.	3.8645	0.59	X X	0.76
6	23.6300	0.12	74.	26.	3.7621	1.68	X X	1.70
7	24.2975	0.24	50.	27.	3.3077	1.15	Bt	1.74
8	25.5625	0.24	56.	27.	3.4819	1.28	X X	1.48
9	26.6625	0.12	4396.	27.	3.3407	100.00	X X	10.96
10	27.4975	0.12	144.	28.	3.2411	3.28	X X	1.20
11	28.0575	0.12	404.	28.	3.1777	9.19	X X	2.51
12	30.9800	0.16	83.	29.	2.8843	1.88	X X	0.91
13	31.7250	0.12	32.	29.	2.8182	0.74	X X	1.17
14	34.7575	0.64	41.	31.	2.5790	0.93	X X	1.41
15	36.5625	0.16	365.	30.	2.4557	8.30	X X	5.13
16	38.3975	0.16	177.	30.	2.3425	4.02	X X	3.09
17	39.4800	0.16	388.	29.	2.2807	8.83	X X	5.62
18	40.3150	0.16	172.	29.	2.2353	3.90	X X	2.69
19	41.1600	0.24	23.	29.	2.1914	0.52	X X	1.15
20	42.4750	0.16	272.	28.	2.1265	6.19	X X	3.16
21	44.6450	0.16	37.	27.	2.0281	0.85	X X	1.12
22	45.8125	0.20	188.	27.	1.9791	4.27	X X	4.27
23	49.2500	0.24	23.	31.	1.8487	0.52	X X	1.12
24	50.1675	0.24	666.	31.	1.8170	15.14	X X	10.47
25	50.6450	0.20	66.	30.	1.8010	1.49	X X	1.41
26	54.8500	0.12	222.	31.	1.6724	5.05	X X	1.45
27	55.3100	0.16	104.	31.	1.6596	2.37	X X	2.00
28	57.2500	0.40	12.	31.	1.6079	0.28	X X	0.78
29	59.9325	0.12	511.	31.	1.5422	11.62	X X	2.19
30	61.6425	0.64	21.	32.	1.5034	0.48	X X	0.85
31	63.9900	0.16	104.	34.	1.4538	2.37	X X	1.65
32	65.0475	0.32	36.	32.	1.4327	0.82	X X	1.10
33	67.7000	0.12	339.	26.	1.3829	7.70	Ot	2.24
34	68.1200	0.08	449.	26.	1.3754	10.22	X	3.16
35	68.2975	0.12	441.	26.	1.3756	10.03	X	1.66

APD 3720 @ LSU Geology Department (DETECTED MASS SPECTROMETER PEAKS)

Listed DI file name	:	DZ2:[200.200]CLO5B.DI
Raw data file name	:	DU:CLO5B.RD;00001
Sample identification	:	*CL-26 R2 340CM*
Measurement date/time	:	6-DEC-90 9:23
Generator settings	:	40 kV, 21 mA
Cu alpha1,2 wavelengths	:	1.54060, 1.54439 ang
Step size, sample time	:	0.040 deg, 1.00 s, 25.00 s/deg
Monochromator used	:	YES
Divergence slit	:	Automatic (Specimen length: 13.0 mm)
Analysis program number	:	2
Peak angle range	:	2.000 - 70.000 deg
Range in D spacing	:	1.34298 - 44.1372 ang
Peak position criterion	:	Top of smoothed data
Cryst peak width range	:	0.00 - 2.00 deg
Minim peak significance	:	0.75
Number of peaks in file	:	36 (Alpha1: 33, Amorphous: 0)
Maximum intensity	:	4529. cts, 4529.3 cps

Peak (no)	Angle (deg)	Tip width (deg)	Peak (cts)	Back g (cts)	D spac (ang)	I/Imax (%)	Type (A1	A2	Ot)	Sign
1	8.9200	0.24	13.	37.	9.9057	0.29	X	X		1.05
2	13.0350	1.60	12.	29.	6.7864	0.26	X	X		1.55
3	20.8825	0.16	745.	29.	4.2505	16.45	X	X		9.55
4	22.0300	0.16	81.	29.	4.0316	1.79	X	X		1.70
5	23.5975	0.16	79.	28.	3.7672	1.75	X	X		1.41
6	24.3150	0.16	59.	28.	3.6576	1.31	X	X		0.95
7	25.6275	0.12	62.	28.	3.4732	1.38	X	X		1.15
8	26.6625	0.12	4529.	28.	3.3407	100.00	X	X		10.72
9	27.4925	0.12	156.	28.	3.2417	3.45	X	X		0.95
10	27.9825	0.12	259.	27.	3.1860	5.72	X	X		1.58
11	29.8675	0.12	49.	27.	2.9891	1.08	X	X		0.87
12	30.4925	0.12	56.	27.	2.9293	1.24	X	X		0.79
13	30.9600	0.16	128.	27.	2.8861	2.82	X	X		2.00
14	34.9540	0.32	45.	25.	2.5655	0.99	X	X		0.83
15	36.5600	0.16	376.	25.	2.4558	8.31	X	X		5.50
16	37.5075	0.56	23.	26.	2.3959	0.51	X	X		1.02
17	38.3525	0.16	123.	26.	2.3451	2.72	X	X		1.70
18	39.4825	0.16	353.	26.	2.2805	7.80	X	X		5.01
19	40.3050	0.12	159.	27.	2.2359	3.51	X	X		1.15
20	41.1375	0.16	31.	27.	2.1925	0.69	X	X		0.91
21	41.7250	0.24	32.	27.	2.1630	0.72	X	X		1.26
22	42.4775	0.16	303.	27.	2.1264	6.68	X	X		3.80
23	45.7925	0.16	196.	28.	1.9799	4.33	X	X		3.31
24	49.2800	0.16	29.	28.	1.8476	0.64	X	X		1.02
25	50.1650	0.20	724.	28.	1.8171	15.98	X	X		9.12
26	50.5850	0.12	85.	27.	1.8030	1.87	X	X		1.10
27	54.8525	0.12	228.	28.	1.6724	5.03	X	X		1.35
28	55.2950	0.12	108.	26.	1.6600	2.39	X	X		1.15
29	59.9375	0.12	552.	27.	1.5421	12.19			Ot	2.63
30	61.7850	1.12	21.	30.	1.5003	0.47	X	X		2.75
31	63.9875	0.12	112.	34.	1.4539	2.48	X	X		1.12
32	64.9925	0.16	64.	34.	1.4338	1.41	X	X		1.00
33	65.7350	0.12	32.	35.	1.4194	0.72	X	X		0.95
34	67.6975	0.12	342.	36.	1.3829	7.56			Ot	2.19
35	68.1200	0.08	441.	36.	1.3754	9.74	X			2.82
36	68.3050	0.12	400.	36.	1.3755	8.83		X		1.55

APD 3720 @ LSU Geology Department (DETECTED MASS SPECTROMETER PEAKS)

Listed DI file name	:	DZ2:[200.200]CLO3B.DI
Raw data file name	:	DU:CLO3B.RD;00001
Sample identification	:	*CL-27 RI 40CM*
Measurement date/time	:	5-DEC-90 11:09
Generator settings	:	40 kV, 21 mA
Cu alpha1,2 wavelengths	:	1.54060, 1.54439 ang
Step size, sample time	:	0.040 deg, 1.00 s, 25.00 s/deg
Monochromator used	:	YES
Divergence slit	:	Automatic (Specimen length: 13.0 mm)
Analysis program number	:	2
Peak angle range	:	2.000 - 70.000 deg
Range in D spacing	:	1.34298 - 44.1372 ang
Peak position criterion	:	Top of smoothed data
Cryst peak width range	:	0.00 - 2.00 deg
Minim peak significance	:	0.75
Number of peaks in file	:	34 (Alpha1: 32, Amorphous: 0)
Maximum intensity	:	4556. cts, 4556.3 cps

Peak (no)	Angle (deg)	Tip width (deg)	Peak (cts)	Back g (cts)	D spac (ang)	I/Imax (%)	Type (A1 A2 Ot)	Sign
1	10.6300	0.16	21.	34.	8.3158	0.46	X X	0.85
2	13.7025	0.64	16.	31.	6.4573	0.35	X X	0.95
3	20.9600	0.16	745.	32.	4.2349	16.36	X X	9.33
4	22.0900	0.16	74.	32.	4.0208	1.62	X X	1.58
5	23.6875	0.20	72.	32.	3.7531	1.59	X X	1.74
6	24.4350	0.12	48.	32.	3.6400	1.04	X X	0.78
7	25.7050	0.24	55.	32.	3.4629	1.20	X X	1.62
8	26.7425	0.12	4556.	32.	3.3309	100.00	X X	10.47
9	27.5625	0.16	190.	32.	3.2336	4.18	X X	2.00
10	28.0800	0.16	256.	32.	3.1752	5.62	X X	2.63
11	29.9325	0.28	53.	31.	2.9828	1.17	X X	1.12
12	31.0275	0.24	76.	29.	2.8800	1.66	X X	2.24
13	32.3575	0.24	14.	31.	2.7645	0.32	X X	1.07
14	34.9475	0.48	41.	31.	2.5654	0.90	X X	1.07
15	35.5350	0.48	35.	31.	2.5243	0.76	X X	0.85
16	36.6450	0.16	357.	30.	2.4503	7.84	X X	4.90
17	38.5375	0.12	119.	30.	2.3342	2.61	X X	0.85
18	39.5600	0.16	388.	29.	2.2762	8.52	X X	5.13
19	40.3800	0.12	193.	29.	2.2319	4.24	X X	1.62
20	41.2500	0.32	23.	29.	2.1868	0.51	X X	0.98
21	45.5575	0.16	282.	28.	2.1226	6.19	X X	3.55
22	45.8800	0.16	199.	27.	1.9763	4.36	X X	3.09
23	50.2450	0.20	734.	34.	1.8144	16.12	X X	7.94
24	54.9300	0.12	250.	29.	1.6702	5.48	X X	1.38
25	55.3875	0.16	106.	29.	1.6575	2.33	X X	1.51
26	57.3150	0.24	16.	28.	1.6062	0.35	X X	1.00
27	59.9975	0.16	538.	26.	1.5407	11.81	X X	5.37
28	61.7800	0.80	20.	29.	1.5004	0.44	X X	0.98
29	64.0550	0.12	121.	31.	1.4525	2.66	X X	1.10
30	65.1150	0.16	44.	32.	1.4314	0.96	X X	0.85
31	65.8250	0.12	37.	34.	1.4177	0.82	X X	0.98
32	67.7775	0.12	380.	35.	1.3815	8.35	Ot	2.14
33	68.1600	0.08	475.	35.	1.3747	10.43	X	4.07
34	68.3600	0.08	467.	35.	1.3745	10.24	X	3.98

APD 3720 @ LSU Geology Department (DETECTED MASS SPECTROMETER PEAKS)

Listed DI file name	:	DZ2:[200.200]CLO7B.DI
Raw data file name	:	DU:CLO7B.RD;00001
Sample identification	:	*CL-30 R2 600CM*
Measurement date/time	:	7-DEC-90 8:52
Generator settings	:	40 kV, 21 mA
Cu alpha1,2 wavelengths	:	1.54060, 1.54439 ang
Step size, sample time	:	0.040 deg, 1.00 s, 25.00 s/deg
Monochromator used	:	YES
Divergence slit	:	Automatic (Specimen length: 13.0 mm)
Analysis program number	:	2
Peak angle range	:	2.000 - 70.000 deg
Range in D spacing	:	1.34298 - 44.1372 ang
Peak position criterion	:	Top of smoothed data
Cryst peak width range	:	0.00 - 2.00 deg
Minim peak significance	:	0.75
Number of peaks in file	:	37 (Alpha1: 36, Amorphous: 0)
Maximum intensity	:	3329. cts, 3329.3 cps

Peak (no)	Angle (deg)	Tip width (deg)	Peak (cts)	Back g (cts)	D spac (ang)	I/Imax (%)	Type (A1 A2 Ot)	Sign
1	6.1225	1.28	11.	41.	14.4242	0.33	x x	0.76
2	8.9700	0.12	42.	38.	9.8506	1.27	x x	1.74
3	12.5125	0.24	14.	35.	7.0686	0.43	x x	0.95
4	13.6700	0.64	15.	32.	6.4725	0.46	x x	0.95
5	15.2900	0.96	10.	29.	5.7902	0.31	x x	0.95
6	19.9150	0.32	52.	27.	4.4547	1.56	x x	1.17
7	20.9425	0.12	543.	28.	4.2384	16.31	x x	3.55
8	22.0875	0.16	72.	30.	4.0212	2.17	x x	1.55
9	23.5950	0.20	67.	32.	3.7676	2.02	x x	1.20
10	24.4175	0.12	69.	34.	3.6425	2.07	x x	1.05
11	25.7400	0.16	67.	35.	3.4583	2.02	x x	0.76
12	26.7225	0.16	3329.	37.	3.3333	100.00	x x	19.95
13	27.5475	0.12	123.	38.	3.2354	3.70	x x	1.78
14	28.0650	0.12	196.	38.	3.1769	5.89	x x	1.17
15	30.5450	0.12	44.	42.	2.9243	1.31	x x	0.95
16	31.0075	0.24	85.	42.	2.8818	2.54	x x	2.88
17	33.1050	0.12	36.	32.	2.7038	1.08	x x	0.91
18	34.9675	0.56	74.	31.	2.5639	2.22	x x	2.40
19	36.6425	0.16	313.	32.	2.4505	9.41	x x	4.68
20	37.7275	0.40	30.	34.	2.3825	0.91	x x	0.85
21	38.5275	0.16	137.	35.	2.3348	4.11	x x	1.74
22	39.5425	0.12	289.	35.	2.2772	8.68	x x	2.04
23	40.3800	0.12	135.	36.	2.2319	4.04	x x	1.35
24	42.5175	0.16	225.	37.	2.1245	6.76	x x	3.55
25	45.8950	0.20	142.	35.	1.9757	4.25	x x	3.47
26	50.2125	0.20	506.	34.	1.8155	15.21	x x	8.91
27	54.9150	0.16	172.	40.	1.6706	5.15	x x	2.51
28	55.3800	0.20	81.	40.	1.6577	2.43	x x	1.58
29	56.3825	0.32	19.	38.	1.6306	0.58	x x	1.05
30	57.3675	0.24	15.	37.	1.6049	0.46	x x	1.23
31	59.9825	0.12	400.	32.	1.5410	12.01	x x	2.14
32	61.6725	0.32	52.	35.	1.5028	1.56	x x	0.76
33	64.0675	0.12	79.	37.	1.4522	2.38	x x	0.78
34	65.0875	0.24	45.	37.	1.4319	1.35	x x	1.82
35	67.7450	0.12	250.	35.	1.3821	7.50	x x	1.78
36	68.1600	0.08	350.	35.	1.3747	10.50	x	2.82
37	68.3600	0.08	324.	35.	1.3745	9.73	x	3.16

APD 3720 @ LSU Geology Department (DETECTED MASS SPECTROMETER PEAKS)

Listed DI file name	:	DZ2:[200.200]CLO1B.DI
Raw data file name	:	DU:CLO1B.RD;00001
Sample identification	:	*CL-46 RI 22 CM*
Measurement date/time	:	6-DEC-90 11:26
Generator settings	:	40 kV, 21 mA
Cu alpha1,2 wavelengths	:	1.54060, 1.54439 ang
Step size, sample time	:	0.040 deg, 1.00 s, 25.00 s/deg
Monochromator used	:	YES
Divergence slit	:	Automatic (Specimen length: 13.0 mm)
Analysis program number	:	2
Peak angle range	:	2.000 - 70.000 deg
Range in D spacing	:	1.34298 - 44.1372 ang
Peak position criterion	:	Top of smoothed data
Cryst peak width range	:	0.00 - 2.00 deg
Minim peak significance	:	0.75
Number of peaks in file	:	31 (Alpha1: 29, Amorphous: 0)
Maximum intensity	:	2916. cts, 2916.0 cps

Peak (no)	Angle (deg)	Tip width (deg)	Peak (cts)	Back g (cts)	D spac (ang)	I/Imax (%)	Type (A1 A2 Ot)	Sign
1	8.770	0.48	12.	45.	10.0748	0.40	x x	1.15
2	13.5375	0.64	11.	32.	6.5356	0.37	x x	0.76
3	19.8175	.032	52.	31.	4.4764	1.78	x x	0.98
4	20.8800	0.16	497.	32.	4.2510	17.05	x x	7.24
5	22.0025	0.16	58.	37.	4.0366	1.98	x x	1.17
6	22.9375	0.40	15.	40.	3.8741	0.52	x x	0.79
7	23.5525	0.16	40.	41.	3.7743	1.36	x x	0.87
8	24.2800	0.24	23.	42.	3.3101	0.79	Bt	0.76
9	26.6600	0.12	2916.	49.	3.3410	100.00	x x	8.71
10	28.0275	0.12	169.	46.	3.1810	5.80	x x	0.79
11	29.9150	0.16	42.	42.	2.9845	1.45	x x	0.87
12	30.9800	0.16	62.	40.	2.8843	2.14	x x	1.32
13	34.9600	0.16	88.	29.	2.5645	3.03	x x	0.78
14	36.5625	0.16	272.	30.	2.4557	9.34	x x	4.07
15	38.4050	0.16	159.	32.	2.3420	5.44	x x	2.63
16	39.4800	0.16	250.	32.	2.2807	8.56	x x	4.07
17	40.3225	0.16	119.	34.	2.2349	4.07	x x	2.09
18	42.4625	0.12	196.	36.	2.1271	6.72	x x	1.26
19	44.6250	0.12	38.	34.	2.0289	1.32	x x	1.29
20	45.7975	0.16	130.	34.	1.9797	4.46	x x	2.19
21	47.3250	0.48	10.	34.	1.9193	0.35	x x	0.78
22	50.1525	0.08	480.	32.	1.8175	16.45	x x	4.57
23	54.8825	0.12	146.	35.	1.6715	5.02	x x	2.51
24	59.9325	0.24	353.	32.	1.5422	12.12	x x	1.91
25	61.6375	0.16	48.	34.	1.5035	1.63	x x	1.70
26	64.0000	0.08	77.	36.	1.4536	2.66	x	1.62
27	65.0250	0.12	48.	36.	1.4332	1.63	x x	1.02
28	65.8025	0.24	18.	36.	1.4181	0.60	x x	1.20
29	68.6850	0.16	237.	36.	1.3832	8.13	x x	3.02
30	68.1200	0.08	331..	35.	1.3754	11.36	x	2.82
31	68.2975	0.12	306.	35.	1.3756	10.50	x	0.95

APPENDIX 1-B
Individual Shoal Volumes

Shoal Number	Isopach Contour Number 0	1	2	3	4	5	6	*Total Vol.*
1	9436768.6	6099564.0	2476081.2	87657.2				
AREA SHOAL 1 (square meters)	9436768.6	6099564.0	2476081.2	30202.7	0.0	0.0	0.0	
VOLUME SHOAL 1 (cubic meters)				117859.9				13441354.4
2	594965.9	63483.8						
AREA SHOAL 2 (square meters)	594965.9	63483.8	0.0	0.0	0.0	0.0	0.0	
VOLUME SHOAL 2 (cubic meters)								376837.7
3	637773.7	124658.2						
AREA SHOAL 3 (square meters)	637773.7	124658.2	0.0	0.0	0.0	0.0	0.0	
VOLUME SHOAL 3 (cubic meters)								474709.6
4	762994.3	51610.5						
AREA SHOAL 4 (square meters)	762994.3	51610.5	0.0	0.0	0.0	0.0	0.0	
VOLUME SHOAL 4 (cubic meters)								446010.3
5	1844612.1	610946.3	38815.3					
AREA SHOAL 5 (square meters)	1844612.1	610946.3	38815.3	0.0	0.0	0.0	0.0	
VOLUME SHOAL 5 (cubic meters)								1581771.5
6	2639127.5	943780.3	232889.1					
AREA SHOAL 6 (square meters)	2639127.5	943780.3	232889.1	0.0	0.0	0.0	0.0	
VOLUME SHOAL 6 (cubic meters)								2554455.4
7	1923992.7	371930.7						
AREA SHOAL 7 (square meters)	1923992.7	371930.7	0.0	0.0	0.0	0.0	0.0	
VOLUME SHOAL 7 (cubic meters)								1426909.7
8	263044.5	56012.0						
AREA SHOAL 8 (square meters)	263044.5	56012.0	0.0	0.0	0.0	0.0	0.0	
VOLUME SHOAL 8 (cubic meters)								201537.3
9	256570.5	56394.5						
AREA SHOAL 9 (square meters)	256570.5	56394.5	0.0	0.0	0.0	0.0	0.0	
VOLUME SHOAL 9 (cubic meters)								198778.4
10	3123820.6	1423642.0	155337.6					
AREA SHOAL 10 (square meters)	3123820.6	1423642.0	155337.6	0.0	0.0	0.0	0.0	
VOLUME SHOAL 10 (cubic meters)								3179724.3
11	857793.2	426673.3	236975.2	46502.8				
AREA SHOAL 11 (square meters)	857793.2	426673.3	236975.2	46502.8	0.0	0.0	0.0	
VOLUME SHOAL 11 (cubic meters)								1150673.6
12	601679.8	417443.1	228982.4	52475.2				
AREA SHOAL 12 (square meters)	601679.8	417443.1	228982.4	52475.2	0.0	0.0	0.0	
VOLUME SHOAL 12 (cubic meters)								1012859.4

Shoal Number	0	1	2	3	4	5	6	*Total Vol.*
13	315502.9	193088.2	93947.1	30822.3				
AREA SHOAL 13 (square meters)	315502.9	193089.2	93949.1	30825.3	0.0	0.0	0.0	
VOLUME SHOAL 13 (cubic meters)								483321.4
14	8284198.5	5781436.3	84039.0	107101.2	17381.9	6193.8		
			224681.4	65337.9	26827.2			
			338213.3					
			220697.6					
			289837.9					
			958247.1					
AREA SHOAL 14 (square meters)	8284198.5	5781436.3	2115716.3	172439.1	44209.1	6193.8	0.0	
VOLUME SHOAL 14 (cubic meters)								12263642.3
15	773267.8	380410.1	95272.5					
AREA SHOAL 15 (square meters)	773267.8	380410.1	95272.5	0.0	0.0	0.0	0.0	
VOLUME SHOAL 15 (cubic meters)								886134.6
16	683450.8	382074.9	162618.7					
AREA SHOAL 16 (square meters)	683450.8	382074.9	162618.7	0.0	0.0	0.0	0.0	
VOLUME SHOAL 16 (cubic meters)								927073.7
17	635285.9	129954.1						
AREA SHOAL 17 (square meters)	635285.9	129954.1	0.0	0.0	0.0	0.0	0.0	
VOLUME SHOAL 17 (cubic meters)								480085.6
18	55719.2	7688.7						
AREA SHOAL 18 (square meters)	55719.2	7688.7	0.0	0.0	0.0	0.0	0.0	
VOLUME SHOAL 18 (cubic meters)								37470.5
19	414154.0	192562.8	42210.5					
AREA SHOAL 19 (square meters)	414154.0	192562.8	42210.5	0.0	0.0	0.0	0.0	
VOLUME SHOAL 19 (cubic meters)								452402.9
20	909418.7	368373.3	27517.0					
AREA SHOAL 20 (square meters)	909418.7	368373.3	27517.0	0.0	0.0	0.0	0.0	
VOLUME SHOAL 20 (cubic meters)								857478.9
21	350299.6	59590.6						
AREA SHOAL 21 (square meters)	350299.6	59590.6	0.0	0.0	0.0	0.0	0.0	
VOLUME SHOAL 21 (cubic meters)								234740.4
22	636289.9	319103.0	118994.9					
AREA SHOAL 22 (square meters)	636289.9	319103.0	118994.9	0.0	0.0	0.0	0.0	
VOLUME SHOAL 22 (cubic meters)								785991.6
23	349088.1	56409.5						
AREA SHOAL 23 (square meters)	349088.1	56409.5	0.0	0.0	0.0	0.0	0.0	
VOLUME SHOAL 23 (cubic meters)								245055.9

Shoal Number	0	1	2	3	4	5	6	*Total Vol.*
24	3209875.8	1936952.1	18981.4	95431.2	33712.6			
			189287.9					
AREA SHOAL 24 (square meters)	3209875.8	1936952.1	208269.3	95431.2	33712.6	0.0	0.0	
VOLUME SHOAL 24 (cubic meters)								3887731.2
25	2636908.0	426391.3	64740.3					
		345597.4						
AREA SHOAL 25 (square meters)	2636908.0	771988.7	64740.3	0.0	0.0	0.0	0.0	
VOLUME SHOAL 25 (cubic meters)								2171368.1
26	514189.7	155685.0						
AREA SHOAL 26 (square meters)	514189.7	155685.0	0.0	0.0	0.0	0.0	0.0	
VOLUME SHOAL 26 (cubic meters)								451701.1
27	412983.0	43810.4						
		19046.8						
AREA SHOAL 27 (square meters)	412983.0	62857.2	0.0	0.0	0.0	0.0	0.0	
VOLUME SHOAL 27 (cubic meters)								285063.0
28	289388.1	89709.1						
AREA SHOAL 28 (square meters)	289388.1	89709.1	0.0	0.0	0.0	0.0	0.0	
VOLUME SHOAL 28 (cubic meters)								256830.4
29	172373.6	44690.5						
AREA SHOAL 29 (square meters)	172373.6	44690.5	0.0	0.0	0.0	0.0	0.0	
VOLUME SHOAL 29 (cubic meters)								142049.9
30	235716.4	77145.2	17009.7					
AREA SHOAL 30 (square meters)	235716.4	77145.2	17009.7	0.0	0.0	0.0	0.0	
VOLUME SHOAL 30 (cubic meters)								216265.5
31	440282.3	223591.6	61183.1					
AREA SHOAL 31 (square meters)	440282.3	223591.6	61183.1	0.0	0.0	0.0	0.0	
VOLUME SHOAL 31 (cubic meters)								520211.6
32	692952.0	367662.4	98937.4					
AREA SHOAL 32 (square meters)	692952.0	367662.4	98937.4	0.0	0.0	0.0	0.0	
VOLUME SHOAL 32 (cubic meters)								837810.2
33	4167665.9	1895598.1	158024.1	87808.9				
		585303.6	358570.9	83482.8				
			374603.0					
AREA SHOAL 33 (square meters)	4167665.9	2480901.7	891198.0	171291.7	0.0	0.0	0.0	
VOLUME SHOAL 33 (cubic meters)								5670047.3
34	627352.8	339446.7	119845.6	36981.9				
AREA SHOAL 34 (square meters)	627352.8	339446.7	119845.6	36981.9	0.0	0.0	0.0	
VOLUME SHOAL 34 (cubic meters)								819196.1

Shoal Number	0	1	2	3	4	5	6	*Total Vol.*
35	9647911.8	7126843.2	1270354.3					
			1912223.5					
AREA SHOAL 35 (square meters)	9647911.8	7126843.2	3182577.8	0.0	0.0	0.0	0.0	
VOLUME SHOAL 35 (cubic meters)								15929021.4
36	3264401.6	602179.3	624716.4	111731.6				
		1160660.5	192331.5					
AREA SHOAL 36 (square meters)	3264401.6	1762839.8	817047.9	111731.6	0.0	0.0	0.0	
VOLUME SHOAL 36 (cubic meters)								4351753.0
37	1426652.9	950258.5	652681.2	387327.8	146817.6			
AREA SHOAL 37 (square meters)	1426652.9	950258.5	652681.2	387327.8	146817.6	0.0	0.0	
VOLUME SHOAL 37 (cubic meters)								2887116.0
38	1098305.6	638951.1	103510.7					
AREA SHOAL 38 (square meters)	1098305.6	638951.1	103510.7	0.0	0.0	0.0	0.0	
VOLUME SHOAL 38 (cubic meters)								1317492.3
39	366559.4	149479.2						
AREA SHOAL 39 (square meters)	366559.4	149479.2	0.0	0.0	0.0	0.0	0.0	
VOLUME SHOAL 39 (cubic meters)								370128.7
40	478455.8	74810.6						
AREA SHOAL 40 (square meters)	478455.8	74810.6	0.0	0.0	0.0	0.0	0.0	
VOLUME SHOAL 40 (cubic meters)								332741.2
41	999666.8	325318.4						
AREA SHOAL 41 (square meters)	999666.8	325318.4	0.0	0.0	0.0	0.0	0.0	
VOLUME SHOAL 41 (cubic meters)								906481.4
42	978935.1	540533.4	157818.6					
AREA SHOAL 42 (square meters)	978935.1	540533.4	157818.6	0.0	0.0	0.0	0.0	
VOLUME SHOAL 42 (cubic meters)								1227274.2
43	899890.2	522482.0	105712.1					
AREA SHOAL 43 (square meters)	899890.2	522482.0	105712.1	0.0	0.0	0.0	0.0	
VOLUME SHOAL 43 (cubic meters)								1104567.2
44	1629314.1	1224599.4	964657.3	648197.8	227721.6	77652.9	25870.8	
AREA SHOAL 44 (square meters)	1629314.1	1224599.4	964657.3	648197.8	227721.6	77652.9	25870.8	
VOLUME SHOAL 44 (cubic meters)								3976889.2
45	11394954.3	7233247.5	493328.7	958846.8	488811.6	224723.8	76059.7	
			215556.0					
			207379.5					
			232471.3					
			1895917.9					
AREA SHOAL 45 (square meters)	11394954.3	7233247.5	3044653.4	958846.8	488811.6	224723.8	76059.7	
VOLUME SHOAL 45 (cubic meters)								17704805.0

Shoal Number	0	1	2	3	4	5	6	*Total Vol.*
46	395168.3	64783.8						
AREA SHOAL 46 (square meters)	395168.3	64784.8	0.0	0.0	0.0	0.0	0.0	
VOLUME SHOAL 46 (cubic meters)								278565.2
47	2255828.9	1331399.6	184351.4					
AREA SHOAL 47 (square meters)	2255828.9	1331399.6	184351.4	0.0	0.0	0.0	0.0	
VOLUME SHOAL 47 (cubic meters)								2689753.3
48	1639700.2	1048537.7	634971.8	98361.5	26594.2			
AREA SHOAL 48 (square meters)	1639700.2	1048537.7	634971.8	98361.5	26594.2	0.0	0.0	
VOLUME SHOAL 48 (cubic meters)								2634963.9
49	44250110.3	65352.8	1087292.1	271194.9	61731.1			
		53114.6	1657971.1	626964.4	154817.9			
		35834246.6	828279.3	68479.1				
		63761.7	1536574.3	565099.3				
		99074.1	7565181.0	202521.8				
		72782.9	536655.6					
		42106.3	68952.7					
		1843963.3						
		178345.8						
AREA SHOAL 49 (square meters)	44250110.3	38252748.1	13280906.1	1734259.5	216549.0	0.0	0.0	
VOLUME SHOAL 49 (cubic meters)								75663655.1
50	1187408.7	481001.2						
AREA SHOAL 50 (square meters)	1187408.7	481001.2	0.0	0.0	0.0	0.0	0.0	
VOLUME SHOAL 50 (cubic meters)								1194955.9
51	594649.1	226552.7	35556.8					
AREA SHOAL 51 (square meters)	594649.1	226552.7	35556.8	0.0	0.0	0.0	0.0	
VOLUME SHOAL 51 (cubic meters)								568323.3
52	3111333.4	2077167.5	416541.1					
			136570.7					
			150390.8					
AREA SHOAL 52 (square meters)	3111333.4	2077167.5	703502.6	0.0	0.0	0.0	0.0	
VOLUME SHOAL 52 (cubic meters)								4512212.5
53	307049.4	41510.3						
AREA SHOAL 53 (square meters)	307049.4	41510.3	0.0	0.0	0.0	0.0	0.0	
VOLUME SHOAL 53 (cubic meters)								205412.6
54	189828.0	65937.3						
AREA SHOAL 54 (square meters)	189828.0	65937.3	0.0	0.0	0.0	0.0	0.0	
VOLUME SHOAL 54 (cubic meters)								177335.6

Shoal Number	0	1	2	3	4	5	6	*Total Vol.*
55	234917.9	90253.2						
AREA SHOAL 55 (square meters)	234917.9	90254.2	0.0	0.0	0.0	0.0	0.0	
VOLUME SHOAL 55 (cubic meters)								230276.7
56	3486106.2	345062.5						
		364618.5						
AREA SHOAL 56 (square meters)	3486106.2	709681.0	0.0	0.0	0.0	0.0	0.0	
VOLUME SHOAL 56 (cubic meters)								2630154.4
57	629064.7	115142.4						
AREA SHOAL 57 (square meters)	629064.7	115142.4	0.0	0.0	0.0	0.0	0.0	
VOLUME SHOAL 57 (cubic meters)								458460.4
58	1172548.7	677319.9	35734.0					
			70789.9					
AREA SHOAL 58 (square meters)	1172548.7	677319.9	106523.9	0.0	0.0	0.0	0.0	
VOLUME SHOAL 58 (cubic meters)								1396749.1
59	2402093.0	298028.8						
AREA SHOAL 59 (square meters)	2402093.0	298028.8	0.0	0.0	0.0	0.0	0.0	
VOLUME SHOAL 59 (cubic meters)								1573582.5
60	1163114.0	100311.8	29859.0					
		118440.7						
AREA SHOAL 60 (square meters)	1163114.0	218752.5	29859.0	0.0	0.0	0.0	0.0	
VOLUME SHOAL 60 (cubic meters)								837633.3
61	3967065.7	221797.9						
		216361.0						
AREA SHOAL 61 (square meters)	3967065.7	438158.9	0.0	0.0	0.0	0.0	0.0	
VOLUME SHOAL 61 (cubic meters)								2531231.5

APPENDIX 1-C
Location Map of Individual Shoals

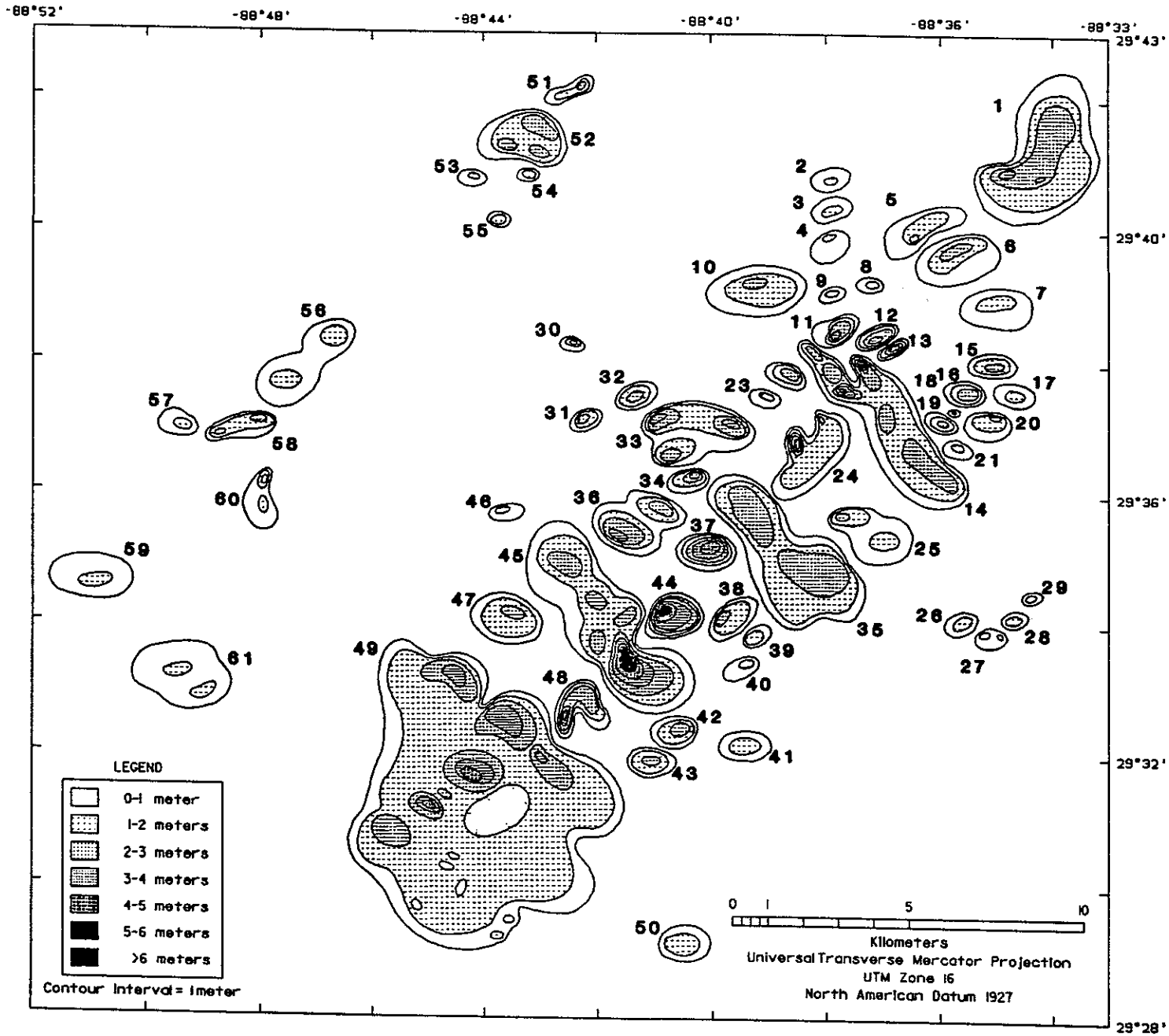
-88°52'
-88°48'
-88°44'
-88°40'
-88°36'
-88°33'
29°43'
29°40'
29°36'
29°32'
29°28'
LEGEND
0-1 meter
1-2 meters
2-3 meters
3-4 meters
4-5 meters
5-6 meters
>6 meters
Contour Interval = 1meter
0 1 5 10
Kilometers
Universal Transverse Mercator Projection
UTM Zone 16
North American Datum 1927